2nd Department of Medicine and Cardiology Center, Medical Faculty,
Albert Szent-Györgyi Clinical Center,
University of Szeged

Focus on atrial function: benefits of three-dimensional speckle-tracking echocardiography

Györgyike Ágnes Piros MD

PhD thesis

Tutor:

Prof. Attila Nemes MD, PhD, DSc

2016

Relevant publications

Full papers

I. Piros GÁ, Domsik P, Kalapos A, Lengyel C, Orosz A, Forster T, Nemes A. Relationships between right atrial and left ventricular size and function in healthy subjects - Results from the three-dimensional speckle tracking echocardiographic MAGYAR-Healthy Study. *Orv Hetil* 2015; 156: 972-978.

II. Piros GÁ, Domsik P, Kalapos A, Lengyel C, Orosz A, Forster T, Nemes A. Left atrial ejection force correlates with left atrial strain and volume-based functional properties as assessed by three-dimensional speckle-tracking echocardiography (from the MAGYAR-Healthy Study). *Rev Port Cardiol* 2016; 35: 83-91. (Impact Factor: 0.454)

III. Nemes A, Piros GÁ, Domsik P, Kalapos A, Lengyel C, Orosz A, Forster T. Correlations between three-dimensional speckle-tracking echocardiography-derived left atrial functional parameters and aortic stiffness in healthy subjects – Results from the MAGYAR-Healthy Study. *Acta Physiol Hung* 2015; 102: 197-205. (Impact factor: 0.734)

IV. Nemes A, Piros GÁ, Lengyel C, Domsik P, Kalapos A, Várkonyi TT, Orosz A, Forster T. Complex evaluation of left atrial dysfunction in patients with type 1 diabetes mellitus by three-dimensional speckle tracking echocardiography: results from the MAGYAR-Path Study. *Anatol J Cardiol* 2016 (in press) (Impact Factor: 0.927)

V. Nemes A, Piros GÁ, Domsik P, Kalapos A, Forster T. Left atrial volumetric and strain analysis by three-dimensional speckle-tracking echocardiography in noncompaction cardiomyopathy – Results from the MAGYAR-Path Study. *Hellenic J Cardiol* 2016; 57: 23-29. (Impact Factor: 1.229)

Abstract

I. Nemes A, Domsik P, Piros GÁ, Kalapos A, Lengyel C, Orosz A, Forster T. Relationships between three-dimensional speckle tracking echocadiography-

derived left atrial functional parameters and aortic stiffness in healthy subjects – Results from the MAGYAR-Healthy Study. *Cardiol Hung* 2015; 45(Suppl D): D80.

Table of contents

Abbreviations

2D – two-dimensional

3D – three-dimensional

2DSTE – two-dimensional speckle-tracking echocardiography

3DS – three-dimensional strain

3DSTE – three-dimensional speckle-tracking echocardiography

AAEF – active atrial emptying fraction

AASV – active atrial stroke volume

AD – aortic distensibility

AP2CH – apical two-chamber view

AP4CH – apical four-chamber view

AS – area strain

ASI – aortic stiffness index

BMI – body mass index

CS – circumferential strain

DBP – diastolic blood pressure

DD – (aortic) diastolic diameter

E and A – diastolic mitral inflow velocities measured by Doppler echocardiography

EDD – end-diastolic diameter

EDV – end-diastolic volume

ESD – end-systolic diameter

ESV – end-systolic volume

EF – ejection fraction

LA – left atrium

LAEFO – left atrial ejection force

LS – longitudinal strain

LV – left ventricular

MA – mitral annulus

MAA – mitral annular area

MAD – mitral annular diameter

MAGYAR – Motion Analysis of the heart and vessels by three-dimensional speckle tracking echocardiography

MV – mitral valve

NCCM – noncompaction cardiomyopathy

PAEF – passive atrial emptying fraction

PASV – passive atrial stroke volume

RA – right atrium

RT3DE – real-time three-dimensional echocardiography

RS – radial strain

RV – right ventricle

SBP – systolic blood pressure

SD – (aortic) systolic diameter

T1DM – type 1 diabetes mellitus

TAEF – total atrial emptying fraction

TASV – total atrial stroke volume

TV – tricuspid valve

SV – stroke volume

Vmax – maximum atrial volume

Vmin – minimum atrial volume

VpreA – pre-contraction atrial volume

1. Introduction

Heart chambers have a complex motion during the heart sycle. While right (RV) and left ventricles (LV) empty through the semilunar pulmonary (PV) and aortic valves (AV) during systole, right (RA) and left atria (LA) behave like a reservoir beside closed mitral (MV) and tricuspid valves (TV). In this phase their chambers enlarge and load from the veins. Following closing of MV and TV in early diastole blood stored in atria flow into the ventricles and atria behave like a conduit in this phase. In late diastole atria become a contractile chamber and eject blood into the ventricles (1).

There is a number of imaging opportunities to assess this complex atrial motion including non-invasive ultrasound examination of the heart. Evaluation of LV dimensions and ejection fraction (EF) is a part of routine echocardiography. However, regarding to complex motion of atria their exact echocardiographic volumetric and functional assessment is relatively difficult due to smaller sizes, disease-related deformations, presence of appendages and veins, etc (2,3). Three-dimensional (3D) echocardiography coupled with speckle tracking capability is a novel approach that might become a powerful methodology for the assessment of LA volumes and function without geometrical assumptions (4,5). Despite basic differences, volumetric real-time 3D echocardiography (RT3DE) and strain-based 3D speckle-tracking echocardiograpy (3DSTE) were found to be comparable, reproducible and interchangeable for quantification of LA dimensions and functional properties (6). Recently, RA volumetric and functional assessment have also been demonstrated using the same methodology (7).

However, physiologic relationship between 3DSTE-derived RA and LV volumes and functional properties have never been assessed in healthy subjects.

There are several aspects of LA function of which relationship with other physiologic parameters were not examined:

3DSTE allows assessment of *different LA functional properties*. In earlier studies 3DSTE was revealed for detailed assessment of all LA features including volumetric measurements (6,8-10), strain assessments (10-12) and calculation of LA ejection force (LAEFO) (13). LA strain and volume-based functional parameters originate from the same 3D dataset, but assessment of LAEFO requires more data including measurement of mitral

annular dimensions and Doppler-derived inflow velocities (14). However, correlations between these LA functional parameters were not examined.

Moreover, there is a strong *interplay between vascular and cardiac mechanics* including arterial-ventricular coupling (18). LV remodeling is a powerful determinant of LA size, therefore arterial stiffness could influence LA dimensions, as well (15-17). Arterial stiffness was found to be associated with LA size in different patient populations (17). However, there is a limited information regarding to interactions between LA and vascular functions in healthy subjects.

Over above mentioned physiologic relationships, specific alterations of different LA features based on 3DSTE-derived analysis are expected:

Type 1 diabetes mellitus (T1DM) is characterized by a progressive destruction of pancreatic beta cells via apoptosis induced by irreversible autoimmune process. LV dysfunction is a known feature in T1DM explained by diabetic microangiopathy affecting small vessels of the heart, progressive fibrosis and cardiac autonomic neuropathy (18). Diastolic dysfunction occurs early at 6 years history of T1DM, whereas systolic dysfunction is later occurring after a mean of 18 years of evolution (18,19). However, 3DSTE-derived detailed analysis of LA functional properties have never been assessed in T1DM.

Noncompaction of the LV myocardium is a rare congenital cardiomyopathy characterized by a distinctive 2-layered appearance of the myocardium due to hypertrabecularization and deep intertrabecular recesses (20). It usually presents with ventricular dysfunction, thromboembolic events and arrhythmias. However, little is known about the behaviour of LA in noncompaction cardiomyopathy (NCCM) (13,21).

2. Aims

To analyze physiological relationships between 3DSTE-derived and routine two-dimensional echocardiographically examined RA morphological and functional parameters in healthy subjects.

To find correlations between LAEFO and 3DSTE-derived LA volume-based functional properties and strain parameters in healthy subjects.

To determine whether correlations exist between 3DSTE-derived LA volume-based and strain parameters characterizing all phasic functions of the LA and echocardiographic aortic elastic properties in healthy subjects.

To compare 3DSTE-derived LA volumetric and strain parameters between T1DM patients and matched healthy controls.

To assess LA volumes and volume- and strain-based functional properties by 3DSTE in NCCM.

3. Methods

Patient population (general considerations). All healthy subjects and patients have been included in the **MAGYAR-Healthy Study** and **MAGYAR-Path Study** (**M**otion **A**nalysis of the heart and **G**reat vessels b**Y** three-dimension**A**l speckle-t**R**acking echocardiography in **Healthy** subjects and in **Path**ological cases). These studies have been organized at the Cardiology Center of the University of Szeged, Hungary to evaluate usefulness, diagnostic and prognostic value of 3DSTE-derived volumetric, strain, rotational etc. parameters in healthy volunteers as well as in pathological cases. In all patients complete 2D Doppler echocardiography study was performed extended with 3DSTE measurements. In healthy volunteers there was no any disease or other condition, which could influence results. Informed consent was obtained from each patient and the study protocol conformed to the ethical guidelines of the 1975 Declaration of Helsinki, as reflected in a priori approval by the institution's human research committee (22).

Biochemical measurements. Blood samples were drawn by venipuncture to evaluate routine blood parameters following 8h fasting including plasma glucose, HbA1c, haematocrit, haemoglobin, creatinine and glomerulus filtration rate (GFR).

Two-dimensional Doppler and tissue Doppler echocardiography. While in the left lateral decubitus position all patients and healthy subjects underwent a complete 2-dimensional (2D) Doppler echocardiography and tissue Doppler study using a commercially available Toshiba Artida^{TM} echocardiography equipment (Toshiba Medical Systems, Tokyo, Japan) with a PST-30SBP phased-array transducer with a center frequency of 3.5 MHz (ranged between 1-5 MHz depending on the necessities and changing automatically). 2D echocardiographic images were obtained in parasternal and apical 4-chamber (AP4CH) and 2-chamber (AP2CH) views. Special care was taken to avoid foreshortening during measurements. All echocardiographic measurements were averaged from 3 beats. LV internal dimensions were measured by M-mode echocardiography using Teichholz method (Figure 1)(2). Significant (> grade 1) valvular regurgitations and stenoses were excluded by Doppler echocardiography. Following Doppler assessment of E/A, the ratio of transmitral E velocity to early diastolic mitral annular velocity (E/E') was measured by tissue Doppler imaging (23). Echocardiographic studies were performed by blinded examiners in respect to the physical status and anamnaesis patients and healthy controls.

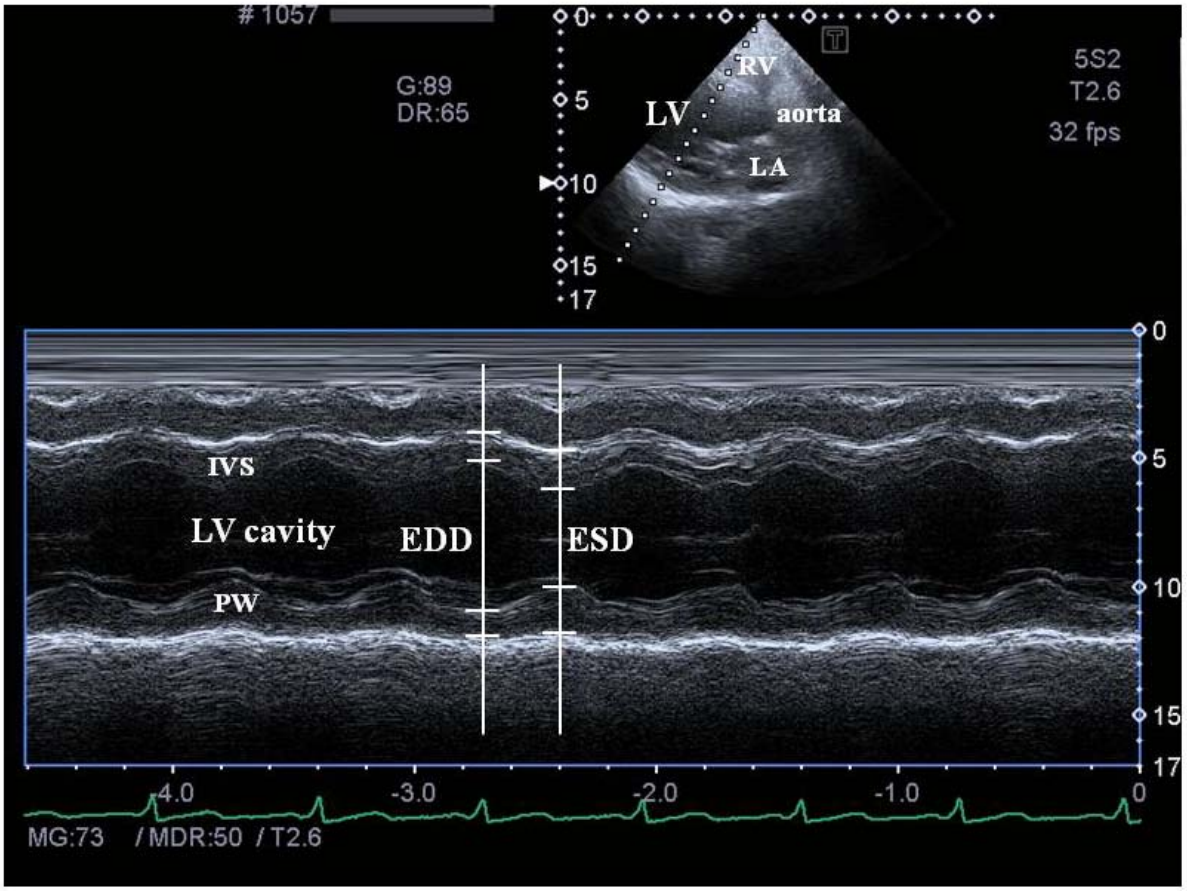

Figure 1 Assessment of left ventricular dimensions in parasternal long-axis view by two-dimensional echocardiography using Techholz-methodology.
Abbreviations: IVS = interventricular septum, EDD and ESD = left ventricular enddiastolic and endsystolic diameter), PW = left ventricular posterior wall, RA = right atrium, RV = right ventricle

Measurement of blood pressure values. Systolic (SBP) and diastolic blood pressure (DBP) values were estimated by a mercury cuff sphygmomanometer following 10 min of rest on the right arm in the supine position (24). The first Korotkoff sound for at least two consecutive heart beats was considered the SBP, while disappearance of fifth Korotkoff sound proved to be the DBP. Coffeinated drinks like coffee, tea, or other types of beverages, and cigarettes were not used or ingested from half and hour before the blood pressure measurements. Data were taken as the average of three consecutive measurements.

Evaluation of aortic stiffness parameters. In the study III, systolic and diastolic ascending aortic diameters (SD and DD, respectively) were recorded in M-mode echocardiography at a level of 3-4 cm above the aortic valve from a parasternal long-axis view as described in more

details in the literature (24,25) (Figure 2). The SD and DD were considered at the time out of maximum aortic anterior motion and at the peak of QRS complex, respectively. All measurements were repeated 3 times, and average data have been given. Echocardiographic aortic elastic properties were calculated using the following equations:

[1] Aortic strain = (SD – DD) / DD

[2] Aortic stiffness index [ASI] = ln (SBP / DBP) / [(SD - DD) / DD], where 'ln' is the natural logarithm.

[3] Aortic distensibility [AD] = 2 x (SD – DD) / [(SBP – DBP) x DD].

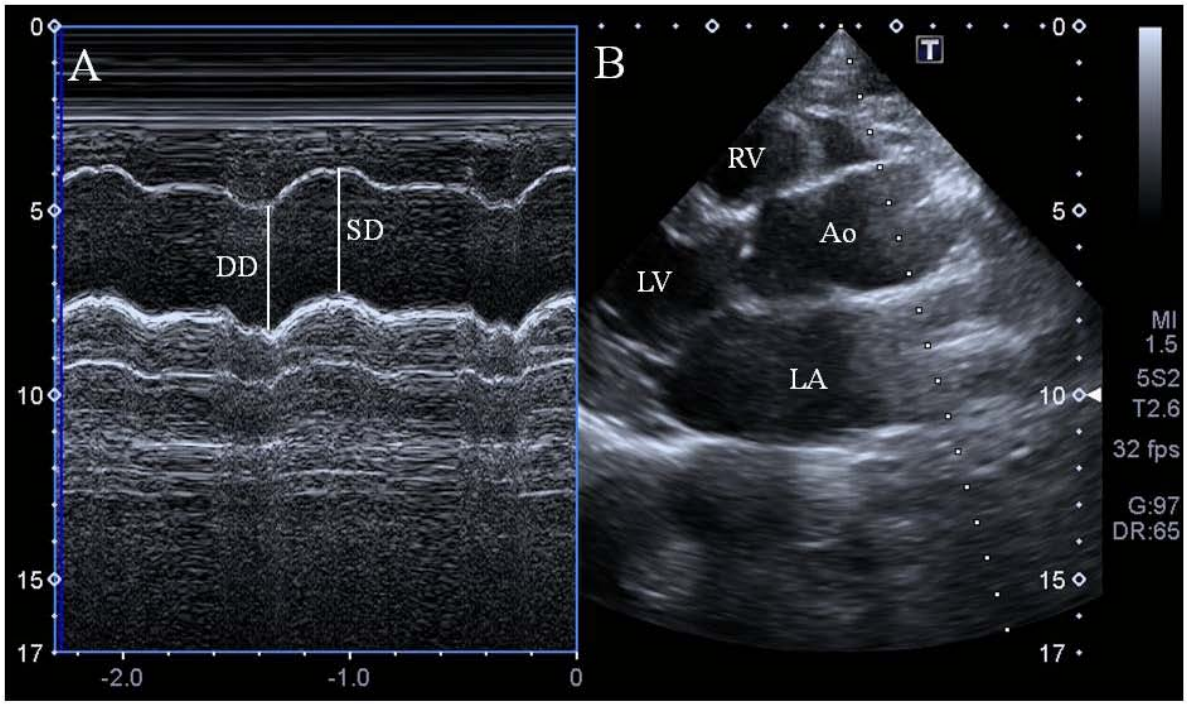

Figure 2. Measurements of systolic (SD) and diastolic (DD) diameters of the ascending aorta (A) are shown on the M-mode tracing obtained at a level 3 cm above the aortic valve (B) at parasternal long-axis view.
Abbreviations: LV = left ventricle, RV = right ventricle, LA = left atrium, Ao = ascending aorta

Three-dimensional speckle-tracking echocardiography. 3D echocardiographic acquisitions were performed using a commercially available fully sampled PST-25SX matrix-array transducer (Toshiba Medical Systems, Tokyo, Japan) by 2 experienced investigators (4,5). Full volume mode was used in which six wedge-shaped subvolumes were acquired over six consecutive cardiac cycles during a single-breathold. Care was taken to avoid movement of the patient or the examination table during acquisitions. The sector width was decreased as much as possible to improve temporal and spatial image resolutions. Pyramidal 3D datasets

were analysed offline using 3D Wall Motion Tracking software version 2.7 (Toshiba Medical Systems, Tokyo, Japan) by experienced investigators. AP4CH and AP2CH views as well as three short-axis views at different levels of the RA/LA (basal, midatrial, and superior regions) were automatically selected by the software from the 3D dataset (Figures 3-4). Following creation of anatomically correct, non-foreshortened optimal views by optimising longitudinal planes in AP4CH and AP2CH views RA/LA boundaries was manually traced starting at the tricuspid/mitral valve level of the RA/LA going toward the RA/LA superior region at end-diastole. Caval veins, RA appendage and coronary sinus were excluded from the cavity during assessments in study I, while pulmonary veins and LA appendage were excluded in studies II-V. The epicardial border was manually adjusted. Subsequently, 3D wall motion tracking was automatically performed through the cardiac cycle.

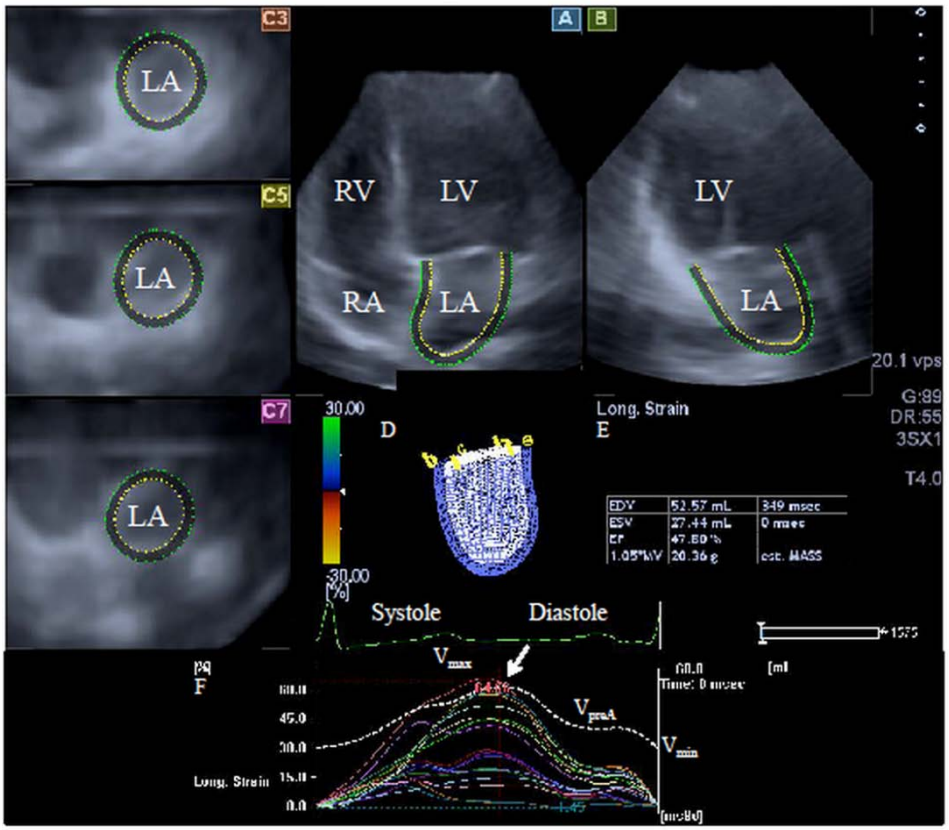

Figure 3 Images from three-dimensional (3D) full-volume dataset showing left atrium (LA) in a patient with type 1 diabetes mellitus is presented: (A) apical four-chamber view, (B) apical two-chamber view, (C3) short-axis view at basal, (C5) mid- and (C7) superior left atrial level. A 3D cast (D), volumetric data (E), time – global volume and time – segmental strain curves (F) of the LA are also presented. Dashed curve (F) represents LA volume changes during cardiac cycle with maximum (V_{max}), minimum (V_{min}) LA volumes and LA volume before atrial contraction (V_{preA}). White arrow represent peak strain (F).

Abbreviations: LA – left atrium, LV left ventricle, RA – right atrium, RV- right ventricle

3DSTE-derived atrial volumetric measurements. From the acquired 3D echocardiographic datasets time – global RA/LA volume change curves were generated from which end-systolic maximum RA/LA volume (V_{max}), end-diastolic minimum RA/LA volume (V_{min}) and early diastolic RA/LA volume before atrial contraction (V_{preA}) were calculated (5) (Figures 2-3). V_{max} and V_{min} were obtained automatically by the software, while V_{preA} was taken from the time – volume change curve (see Figures 3-4).

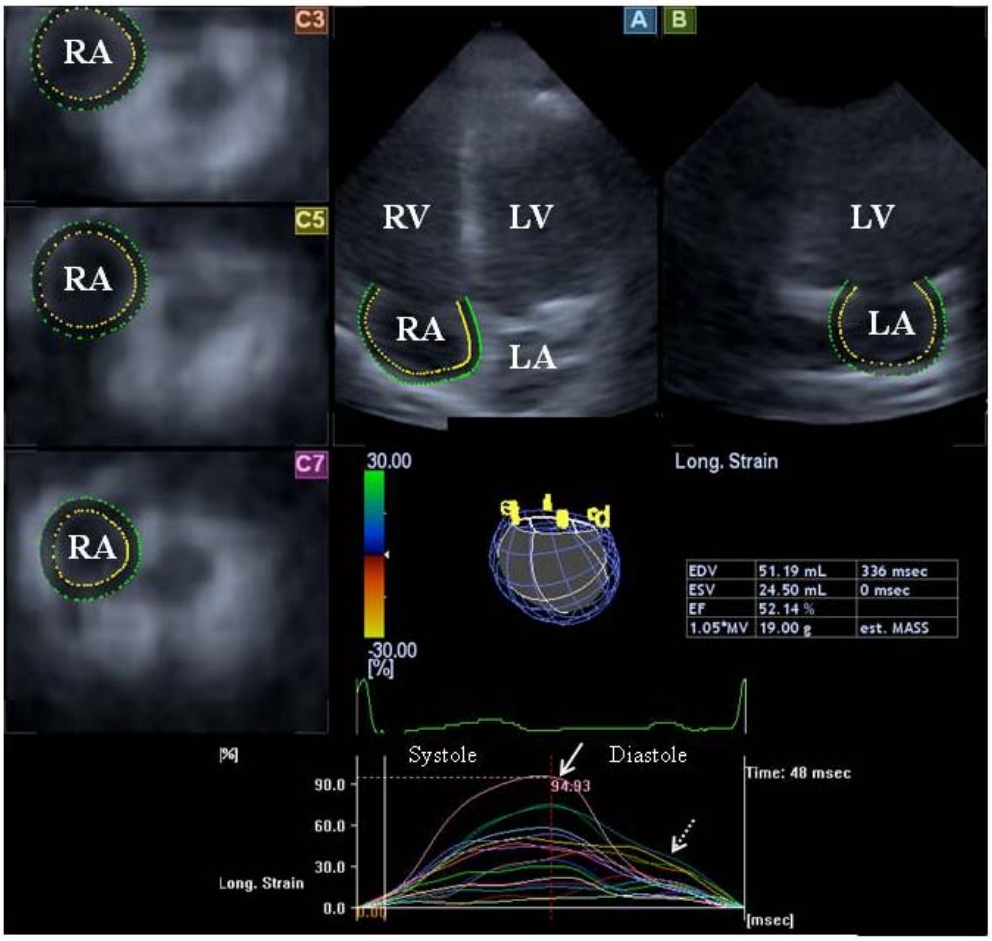

Figure 4 Images from three-dimensional (3D) full-volume dataset showing right atrium (RA) in a healthy subject is presented: (A) apical four-chamber view, (B) apical two-chamber view, (C3) short-axis view at basal, (C5) mid- and (C7) superior RA atrial level. A 3D cast, volumetric data, time – segmental strain curves of the RA are also presented. White arrow represent peak segmental strains, while dashed arrow represents strains at atrial contraction.
Abbreviations: LA – left atrium, LV left ventricle, RA – right atrium, RV- right ventricle

From the three volumes several measurements were selected as indices of RA/LA function as demonstrated in Table 1 (5):

Table 1 The way to calculate atrial stroke volumes and emptying fractions in each phasis of left atrial motion is presented

Functions	**Stroke volumes (ml)**	**Emptying fractions (%)**
Reservoir	**Total atrial SV = V_{max}-V_{min}**	**Total atrial EmF= Total atrial SV/ V_{max}**
Conduit function	**Passive atrial SV= V_{max} -V_{preA}**	**Passive atrial EmF= Passive atrial SV/ V_{max}**
Active contraction	**Active atrial SV= V_{preA}- V_{min}**	**Active atrial EmF= Active atrial SV/V_{preA}**

Abbreviations: EF = emptying fraction, SV = stroke volume, V_{max} = maximum left atrial volume, V_{min} = minimum left atrial volume, V_{preA} = left atrial volume before atrial contraction

3DSTE-derived atrial strain assessments. Form the same 3D echocardiographic datasets time curves of segmental unidirectional radial (RS), longitudinal (LS), circumferential (CS) and complex area (AS) and (3DS) strains were generated using the 16-segment model obtained for the LV (4,5,26,27):

[1] LS = strain in the direction parallel to the endocardial contour

[2] CS = fiber shortening along the circular perimeter, strain in the circumferential direction

[3] RS = radially directed deformation, strain in the perpendicular direction

[4] 3DS = strain in the wall thickening direction, combination of radial, circumferential and longitudinal strains, and

[5] AS = ratio of endocardial area change during the cardiac cycle, percentage change in area

On each time – segmental strain curve peak strains characterizing LA reservoir function were measured. Global strains were calculated by the software taking into consideration the whole RA/LA, while mean segmental strains were obtained as the average of strains of 16 segments. The software calculated these parameters automatically (Figures 2-3).

3DSTE for left atrial ejection force measurements. There is a third way to analyse LA function by calculating LAEFO. According to the Newton's second law of motion, the force generated by the LA in LA active contraction phase could be calculated using the following equation: LAEFO = 0.5 × 1.06 × (MAD or MAA) × V^2, where 0.5 is a coefficient factor, 1.06 g/cm^3 is the blood density and V is the peak A wave velocity (28). From the same 3D echocardiographic dataset, mitral annulus (MA) could be obtained by optimizing cross-sectional planes on the endpoints of the MA in the AP4CH and AP2CH views (Figure 5)(13). MA diameter (MAD) was then defined as the perpendicular line drawn from the top of the MA curvature to the middle of the straight MA border, while MA area (MAA) could also be measured using planimetry. For the evaluation of LAEFO, diastolic MAD and MAA data were used.

Stastical analysis. Statistical analyses were performed using the MedCalc software (MedCalc, Mariakerke, Belgium). All continuous variables are expressed as mean ± standard deviation. Statistical significance was determined as a *p* value of less than 0.05. The Shapiro-Wilk test was used to check the normality of data. Independent samples Student *t* test were used to compare continuous variables. Chi-square analysis and Fisher's exact test were used for comparison of categorical variables. Pearson's coefficient was used for intra- and interobserver correlations. Intra- and interobserver agreements were studied according to Bland and Altman method (29).

Figure 5 From three-dimensional echocardiographic dataset, the mitral annulus (MA) could be obtained by optimizing cross-sectional planes on the apical 4-chamber (A) and 2-chamber (B) views demonstrating an optimal MA image on cross-sectional view (C7). Using Doppler-derived mitral inflow peak A wave velocity, the left atrial ejection force (LAEFO) could be calculated.

Abbreviations: E and A = Doppler-derived mitral inflow velocities, LA = left atrium, LV = left ventricle, MA = mitral annulus, RA = right atrium, RV = right ventricle

4. Results

4.1. Relationships between right atrial and left ventricular size and function in healthy subjects

Patient population. The study comprised 20 randomly selected healthy subjects (mean age: 37.1 ± 10.3 years, 12 men), who were examined by routine 2D Doppler echocardiography and 3DSTE. None of the cases had any disease or pathological factor which could affect results.

Clinical, routine 2D echocardiographic and 3DSTE data are presented in Tables 2-4.

Table 2 Clinical and two-dimensional echocardiographic data

	values
Patients number	20
Age (years)	37.1 ± 10.3
Male gender (%)	12 (60)
BMI (kg/m^2)	24.6 ± 3.0
Two-dimensional echocardiography	
LA diameter (from parasternal long-axis view) (mm)	32.9 ± 3.2
LV end-diastolic diameter (mm)	47.2 ± 6.6
LV end-diastolic volume (ml)	96.1 ± 16.3
LV end-systolic diameter (mm)	29.4 ± 4.3
LV end-systolic volume (ml)	32.7 ± 10.9
Interventricular septum (mm)	9.6 ± 2.0
LV posterior wall (mm)	9.6 ± 2.4
LV ejection fraction (%)	66.6 ± 7.6
E/A	1.33 ± 0.16

Abbreviations: LV = left ventricle, LA = left atrium, BMI = body mass index

Table 3 Three-dimensional speckle tracking echocardiography-derived right atrial volumes and volume-base functional properties

	Values
Calculated right atrial volumes	
V_{max} (ml)	37.54 ± 9.45
V_{min} (ml)	23.18 ± 7.35
V_{preA} (ml)	30.27 ± 8.27
Right atrial stroke volumes	
TASV (ml)	14.85 ± 4.68
PASV (ml)	8.08 ± 4.51
AASV (ml)	6.77 ± 3.17
Right atrial emptying fractions	
TAEF (%)	38.82 ± 8.30
PAEF (%)	20.61 ± 9.14
AAEF (%)	22.47 ± 10.15

Abbreviations: AAEF = active atrial emptying fraction, AASV = active atrial stroke volume, PAEF = passive atrial emptying fraction, PASV= passive atrial stroke volume, TAEF = total atrila emptying fraction, TASV = total atrial stroke volume, V_{max} = maximum right atrial volume, V_{min} = minimum right atrial volume, V_{preA} = right atrial volume before atrial contraction

Relationships between LV-EF and 3DSTE-derived RA parameters. LVEF significantly correlated with systolic V_{max} (r =-0.44, p =0.05) and diastolic V_{preA} (r =-0.44, p =0.05). Relationships could not be detected between volume-based functional parameters and LVEF. LVEF showed significant correlations with diastolic AS at atrial contraction (r =0.42, p =0.05).

Table 4 Three-dimensional speckle tracking echocardiography-derived global peak strains and strains at atrial contraction in healthy subjects

	Peak strains	Strains at atrial contraction
Radial strain (%)	-14.84 ± 9.23	-7.28 ± 8.00
Circumferential strain (%)	11.78 ± 7.83	8.93 ± 9.94
Longitudinal strain (%)	30.19 ± 10.80	8.68 ± 9.21
3D strain (%)	-6.43 ± 5.38	-4.54 ± 4.84
Area strain (%)	40.72 ± 18.87	16.09 ± 16.15

Abbreviation: 3D = three-dimensional

Relationships between LV end-systolic parameters and 3DSTE-derived RA properties. LV end-systolic diameter (ESD) correlated with V_{max} (r =0.48, p =0.03), V_{min} (r =0.43, p =0.05) and V_{preA} (r =0.52, p =0.02). LV end-systolic volume (ESV) showed significant correlations with V_{preA} (r =0.50, p =0.02), while tendentious relationships could be shown with V_{max} (r =0.42, p=0.07) and V_{min} (r =0.40, p =0.08). LV-ESD did not show correlation with any of RA volume-based functional parameters. Significant correlations could be detected between LV-ESV and AASV (r =0.49, p =0.03). While LV-ESD correlated with RS at atrial contraction (r =-0.47, p =0,04), LV-ESV did not correlate with any of strain parameters.

Relationships between LV end-diastolic parameters and 3DSTE-derived RA properties. LV end-diastolic diameter and volume (EDD and EDV) did not show relationship with RA volumes and volume-based functional parameters. While LV-EDD significantly correlated with LS at atrial contraction (r =0.48, p =0.03), CS at atrial contraction (r =0.45, p =0.05) and 3DS at atrial contraction (r =-0.43, p =0.05), and correlation tendencies were shown with peak AS (r =-0.40, p =0.08), LV-EDV did not shown relationship with any functional parameters.

4.2. Correlations between left atrial ejection force and left atrial strain and volume-based functional properties in healthy subjects

Patient population. The study group consisted of 34 healthy subjects (mean age: 36.1 ± 11.2 years, 15 men) in sinus rhythm. None of them had known disease or any factor which could theoretically affect results.

Clinical and echocardiographic data. Baseline clinical and echocardiographic data of healthy subjects are presented in Table 5. All 2D echocardiographic and 3DSTE-derived data were in normal range in this healthy population.

Left atrial functional parameters. 3DSTE-derived volume-based and strain parameters characterizing all phases of LA function together with LAEFO are presented in Table 6.

Correlations. Both MAD- and MAA-based LAEFO showed correlations with global 3D strain at atrial contraction. Moreover, $LAEFO_{MAD}$ correlated with AAEF, as well (Table 7). Despite LAEFO is a characteristics of LA booster pump function, correlations could be demonstrated between LAEFO and volume-based and strain characteristics of LA reservoir function, as well (global peak strains, TASV and TAEF). No correlations could be demonstrated between LAEFO and parameters characterizing LA conduit function (PASV, PAEF).

Table 5. Clinical, two-dimensional and three-dimensional speckle tracking echocardiographic data of subjects

	data
Age (years)	36.1 ± 11.2
Male gender (%)	15 (44)
2D echocardiography	
LA diameter (parasternal long-axis view)	33.5 ± 3.7
LV end-diastolic diameter (mm)	47.0 ± 6.5
LV end-diastolic volume (ml)	99.3 ± 24.6
LV end-systolic diameter (mm)	30.3 ± 4.6
LV end-systolic volume (ml)	36.2 ± 13.3
Interventricular septum (mm)	9.7 ± 1.9
LV posterior wall (mm)	10.1 ± 2.1
LV ejection fraction (%)	63.7 ± 8.2
mitral E wave	74.6 ± 19.7
mitral A wave	57.9 ± 11.5
E/A	1.44 ± 0.31
E/E’	6.21 ± 1.75
3D speckle tracking echocardiography	
Maximum LA volume (V_{max}) (ml)	36.6 ± 6.6
Minimum LA volume (V_{min}) (ml)	16.5 ± 5.0
Pre-atrial contraction LA volume (V_{preA}) (ml)	24.1 ± 6.2
End-diastolic mitral annular diameter (cm)	2.68 ± 0.31
End-systolic mitral annular diameter (cm)	2.06 ± 0.42
End-diastolic mitral annular area (cm^2)	8.20 ± 1.75
End-systolic mitral annular area (cm^2)	4.70 ± 0.88

Abbreviation. 2D = two-dimensional 3D = three-dimensional, LA = left atrial, LV = left ventricular

Table 6. Characteristics of left atrial function

Systole	**Reservoir function**	
Strains	global peak radial strain (%) global peak circumferential strain (%) global peak longitudinal strain (%) global peak 3D strain (%) global peak area strain (%)	-19.4 ± 8.5 32.4 ± 14.1 27.5 ± 7.7 -11.9 ± 7.3 67.2 ± 25.6
Volume-based functional properties	total atrial stroke volume (ml) total atrial emptying fraction (%)	20.2 ± 5.0 55.2 ± 10.7
Diastole	**Conduit function**	
Volume-based functional properties	passive atrial stroke volume (ml) passive atrial emptying fraction (%)	12.6 ± 4.7 34.4 ± 11.2
Diastole	**Active contraction**	
Strains	global radial strain at atrial contraction (%) global longitudinal strain at atrial contraction (%) global circumferential strain at atrial contraction (%) global 3D strain at atrial contraction (%) global area strain at atrial contraction %)	-7.7 ± 7.4 7.7 ± 6.9 10.8 ± 10.1 -6.0 ± 5.2 17.6 ± 15.2
Volume-based functional properties	active atrial stroke volume (ml) active atrial emptying fraction (%)	7.6 ± 2.8 31.9 ± 9.2
Ejection forces	left atrial ejection force based on mitral anular diameter (kdyne) left atrial ejection force based on mitral anular area (kdyne)	5.0 ± 2.1 15.2 ± 7.0

Abbreviation. 3D = three-dimensional

Table 7. Correlations between LA ejection force and other characteristics of LA function

LA function	Parameters	Correlation coeffient with $LAEFO_{MAD}$	Correlation coeffient with $LAEFO_{MAA}$
Reservoir (Systole)	peak radial strain	-0.22 (p =0.23)	-0.10 (p =0.58)
	peak circumferential strain	**0.39 (p =0.02)**	0.29 (p =0.11)
	peak longitudinal strain	**0.32 (p =0.05)**	0.24 (p =0.18)
	peak 3D strain	-0.14 (p =0.44)	-0.07 (p =0.69)
	peak area strain	**0.43 (p =0.01)**	0.31 (p =0.07)
	total atrial stroke volume	**0.30 (p =0.05)**	**0.31 (p =0.05)**
	total atrial emptying fraction	**0.31 (p =0.05)**	0.25 (p =0.15)
Conduit (Diastole)	passive atrial stroke volume	0.18 (p =0.33)	0.26 (p =0.15)
	passive atrial emptying fraction	0.10 (p =0.40)	0.14 (p =0.45)
Active contraction (Diastole)	radial strain at atrial contraction (%)	-0.26 (p =0.15)	-0.20 (p =0.26)
	circumferential strain at atrial contraction (%)	0.21 (p =0.26)	0.18 (p =0.34)
	longitudinal strain at atrial contraction (%)	-0.12 (p =0.54)	-0.17 (p =0.37)
	3D strain at atrial contraction (%)	**-0.44 (p =0.01)**	**-0.37 (p =0.03)**
	area strain at atrial contraction %)	0.18 (p =0.32)	0.13 (p =0.50)
	active atrial stroke volume	0.26 (p =0.15)	0.28 (p =0.12)
	active atrial emptying fraction	**0.36 (p =0.04)**	0.27 (p =0.12)

Abbreviation. 3D = three-dimensional, LA = left atrial

Reproducibility of MAD and MAA measurements. Reproducibility measurements were performed in 17 healthy controls. The mean ± standard deviation difference in values obtained by two observers for the measurements of 3DSTE-derived diastolic and systolic MAD and diastolic and systolic MAA were -0.02 ± 0.43 cm, 0.02 ± 0.43 cm, -0.06 ± 1.49 cm^2 and 0.07 ± 1.02 cm^2, respectively. Correlation coefficients between measurements of 2 observers were 0.77, 0.79, 0.89 and 0.89 (p =0.0003, 0.0002, <0.0001 and <0.0001), respectively (Figures 6-9) (interobserver agreement). The mean ± standard deviation difference in values obtained by 2 mesurements of the same observer for 3DSTE-derived diastolic and systolic MAD and diastolic and systolic MAA were 0.03 ± 0.38 cm, -0.01 ± 0.34 cm, 0.05 ± 0.87 cm^2, and 0.04 ± 0.97 cm^2, respectively. Correlation coefficient between these independent measurements of the same observer were 0.78, 0.83, 0.96 and 0.90 (p =0.0002, <0.0001, <0.0001 and <0.0001), respectively (Figures 6-9) (intraobserver agreement).

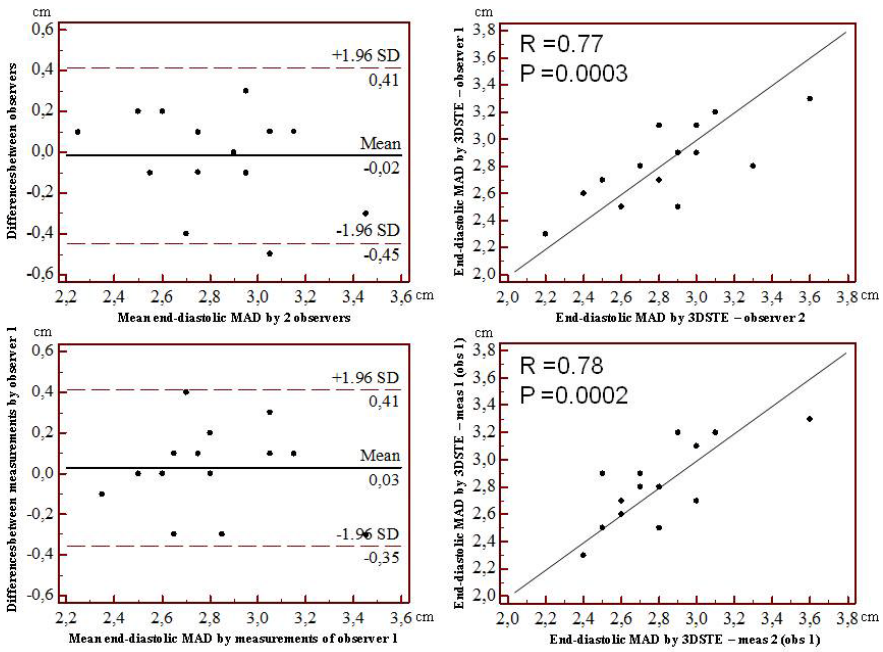

Figure 6 Interobserver (upper graphs) and intraobserver (lower graphs) agreements and correlations for measuring end-diastolic MAD by three-dimensional speckle-tracking echocardiography are presented.
Abbreviations: 3DSTE = three-dimensional speckle-tracking echocardiography, MAD = 3DSTE-derived mitral annulus area

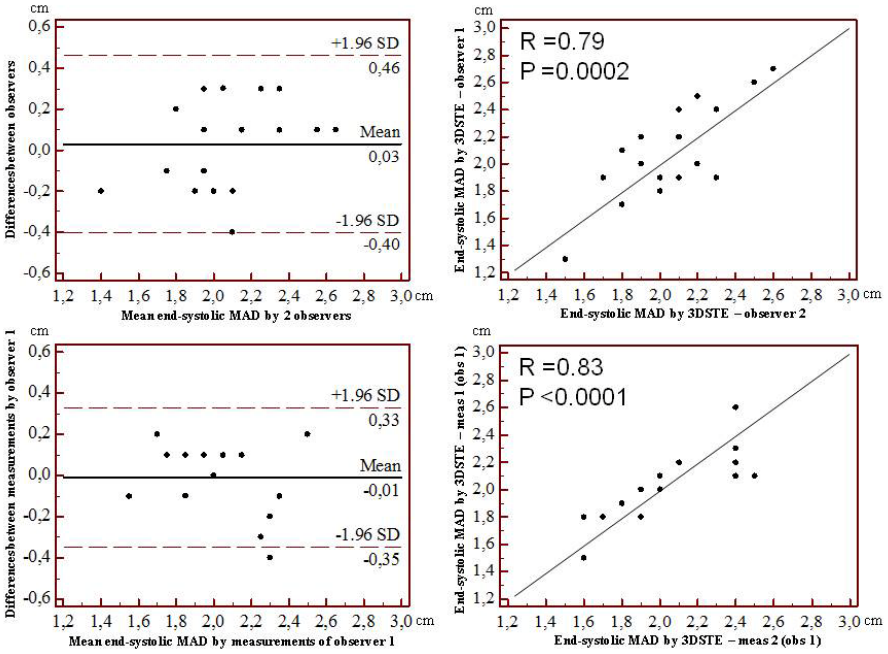

Figure 7 Interobserver (upper graphs) and intraobserver (lower graphs) agreements and correlations for measuring end-systolic MAD by three-dimensional speckle-tracking echocardiography are presented.
Abbreviations: 3DSTE = three-dimensional speckle-tracking echocardiography, MAD = 3DSTE-derived mitral annulus area

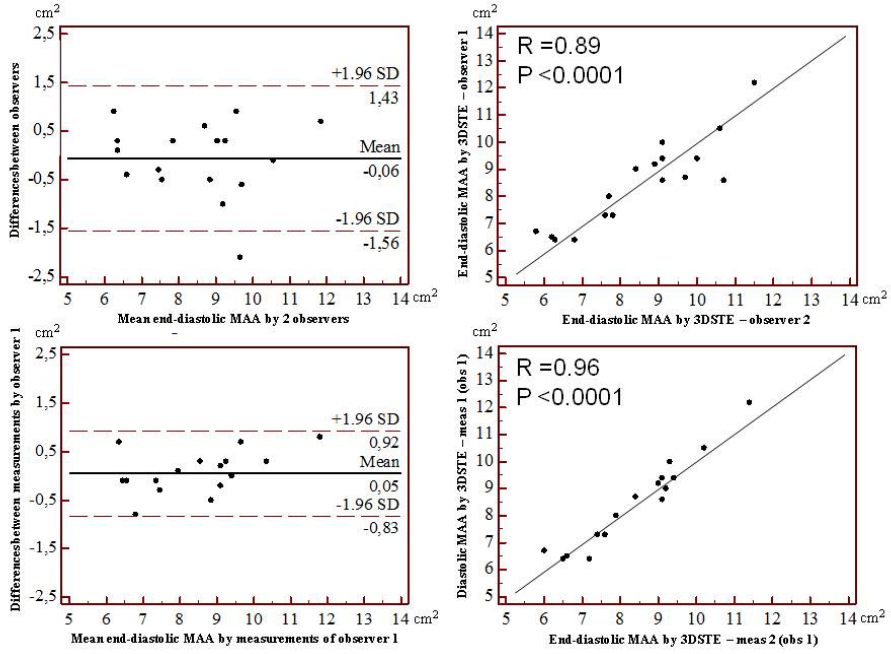

Figure 8 Interobserver (upper graphs) and intraobserver (lower graphs) agreements and correlations for measuring end-diastolic MAA by three-dimensional speckle-tracking echocardiography are presented.
Abbreviations: 3DSTE = three-dimensional speckle-tracking echocardiography, MAA = 3DSTE-derived mitral annulus area

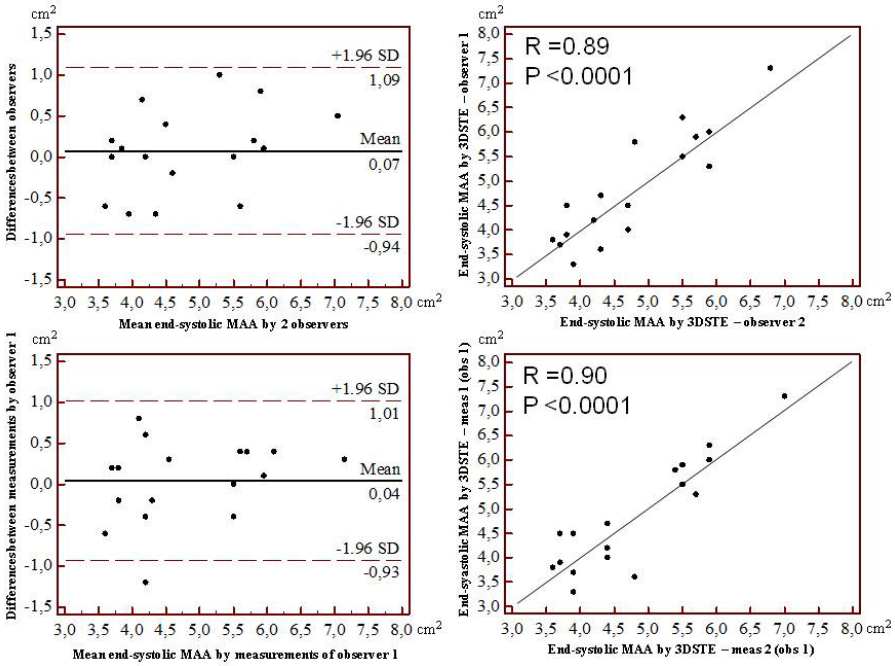

Figure 9 Interobserver (upper graphs) and intraobserver (lower graphs) agreements and correlations for measuring end-systolic MAA by three-dimensional speckle-tracking echocardiography are presented.
Abbreviations: 3DSTE = three-dimensional speckle-tracking echocardiography, MAA = 3DSTE-derived mitral annulus area

4.3. Correlations between left atrial functional parameters and aortic stiffness in healthy subjects

Patient population. The study included 19 healthy volunteers (mean age: 37.9 ± 11.4 years, 11 men) who had undergone complete 2D Doppler transthoracic echocardiography extended with echocardiographic aortic elastic properties assessments. 3DSTE has also been performed following 2D echocardiography in all cases. None of the subjects had any known disease which could have affected results.

Two-dimensional echocardiographic data. Routine 2D echocardiographic LV and LA data and aortic elastic properties are summarized in Table 8.

Table 8 Two-dimensional echocardiographic data and aortic elastic properties of subjects

	Data
Left ventricular diastolic diameter (mm)	48.0 ± 6.8
Left ventricular systolic diameter (mm)	30.1 ± 4.2
Left ventricular diastolic volume (ml)	100.7 ± 20.2
Left ventricular systolic volume (ml)	34.8 ± 11.0
Interventricular septum (mm)	9.5 ± 2.0
Left ventricular posterior wall (mm)	9.5 ± 2.3
Left ventricular ejection fraction (%)	65.7 ± 7.0
Systolic aortic diameter (mm)	30.3 ± 3.6
Diastolic aortic diameter (mm)	26.8 ± 3.8
Systolic minus diastolic aortic diameter (mm)	3.50 ± 2.28
Aortic strain	0.13 ± 0.09
Aortic distensibility (cm^2/dynes 10^{-6})	4.58 ± 3.21
Aortic stiffness index	5.17 ± 3.45

Three-dimensional speckle-tracking echocardiographic data. 3DSTE-derived volumes, volume-based functional properties and strain parameters are summarized in Tables 9-10.

Table 9 Comparison of 3DSTE-derived volumetric and volume-based functional left atrial parameters in patients with type 1 diabetes mellitus and controls

	Data
Calculated volumes (ml)	
Maximum left atrial volume (V_{max})	35.6 ± 6.4
Minimum left atrial volume (V_{min})	16.3 ± 4.9
left atrial volume before atrial contraction (V_{preA})	23.8 ± 6.7
Stroke volumes (ml)	
Total atrial stroke volume	19.3 ± 4.5
Passive atrial stroke volume	11.8 ± 4.7
Active stroke volume	7.5 ± 3.2
Emptying fractions (%)	
Total atrial emptying fraction	54.5 ± 10.2
Passive atrial emptying fraction	33.5 ± 12.3
Active atrial emptying fraction	31.4 ± 9.2

Correlations (volumetric data vs. aortic elastic properties). None of atrial volumes correlated with echocardiographic aortic elastic properties. Active atrial stroke volume correlated with ASI (r =0.45, p =0.05), while passive atrial stroke volume tended to be correlated with ASI (r =-0.42, p =0.09). None of other volume-based functional properties correlated with any of aortic stiffness parameters.

Correlations (peak strains vs. aortic elastic properties). Global peak 3D strain correlated with aortic strain (r =-0.46, p =0.05). Only tendentious correlations could be demonstrated between global radial peak strain and ASI (r =-0.39, p =0.08) and aortic strain (r =-0.41, p =0.07) and between mean segmental longitudinal peak strain and aortic strain (r =0.41, p =0.08).

Table 10 Comparison of 3DSTE-derived global and mean segmental peak strains and strains at atrial contraction in healthy subjects

	Peak strain	Strain at atrial contraction
Global strain parameters		
Radial strain (%)	-21.8 ± 11.8	-8.5 ± 8.3
Circumferential strain (%)	28.7 ± 10.0	10.7 ± 11.4
Longitudinal strain (%)	24.2 ± 6.6	9.0 ± 9.4
Area strain (%)	57.7 ± 17.6	16.5 ± 16.5
3D strain (%)	-13.9 ± 10.8	-5.3 ± 5.4
Mean segmental strain parameters		
Radial strain (%)	-23.1 ± 9.0	-8.6 ± 5.5
Circumferential strain (%)	36.6 ± 12.4	13.3 ± 10.0
Longitudinal strain (%)	31.6 ± 6.7	9.2 ± 6.2
Area strain (%)	74.5 ± 23.2	21.2 ± 15.1
3D strain (%)	-16.4 ± 6.8	-6.7 ± 5.0

Abbreviations: 3D = three-dimensional

Correlations (strains at atrial contraction vs. aortic elastic properties). Global radial strain at atrial contraction correlated with ASI ($r = -0.49$, $p = 0.04$) and aortic strain ($r = -0.50$, $p = 0.04$) and tended to be correlated with AD ($r = 0.43$, $p = 0.07$).

4.4. Complex evaluation of left atrial dysfunction in patients with type 1 diabetes mellitus

Patient population. This prospective study consists of 17 subcutaneous insuline pumpe-treated non-obese patients with T1DM (mean age: 33.5 ± 8.2 years, 8 males, duration of T1DM: 17.0 ± 11.1 years, body mass index: 23.3 ± 3.0 kg/m^2, daily insulin dose: 39.0 ± 7.3 IU). To exclude possible cardiovascular disease, patients with complaints of chest pain, dyspnea or signs of cerebral or peripheral artery disease were not included. Their results were compared to 20 age- and gender-matched healthy controls (mean age: 36.9 ± 11.0 years, 9 males, body mass index: 23.1 ± 1.2 kg/m^2). Presence of any disorder which might presumable influence the results were excluded from the healthy controls.

Demographic, biochemical and two-dimensional echocardiographic data. Hypertension and hypercholesterolaemia were frequent in T1DM patients. No significant differences were demonstrated in standard echocardiographic parameters between groups (Table 11). While fasting plasma glucose (5.3 ± 0.6 mmol/l vs. 5.1 ± 0.8 mmol/l, p =0.93), creatinine (75 ± 5 umol/l vs. 78 ± 3 umol/l, p =0.91), haematocrit (41 ± 2% vs. 40 ± 1%, p =0.90) and haemoglobin (134 ± 3 mmol/l vs. 132 ± 4 mmol/l, p =0.88) levels did not differ between T1DM patients and controls and GFR >60 ml/min/1.73 m^2 could be measured in both groups, HbA1c proved to be significantly increased in T1DM patients (8.1 ± 1.5% vs. 5.2 ± 1.0%, p <0.05). These results suggest that anaemia or impaired renal function could not be confirmed in this T1DM patient population.

3DSTE-derived volumes and volume-based functional properties. Significantly increased LA maximum (45.2 ± 10.3 ml vs. 35.9 ± 6.3 ml, p =0.002), LA minimum (21.6 ± 6.3 ml vs. 16.3 ± 4.8 ml, p =0.006) volumes and LA volume before atrial contraction (31.5 ± 9.1 ml vs. 24.0 ± 6.6 ml, p =0.006) could be detected in T1DM patients as compared to controls. Total atrial stroke volume (SV) proved to be increased (23.6 ± 6.9 ml vs. 19.6 ± 4.6 ml, p =0.04) in patients with T1DM. Other volume-based LA functional properties showed no significant differences between groups (Figure 10).

Table 11 Baseline demographic and two-dimensional echocardiographic data in patients with type 1 diabetes mellitus and controls

	Type 1DM patients (n=17)	Controls (n=20)	p-value
Risk factors			
Age, years	33.5 ± 8.2	36.9 ± 11.0	0.15
Male gender, %	8 (47)	9 (45)	1.00
Hypertension, %	4 (24)	0 (0)	0.04
Hypercholesterolaemia, %	4 (24)	0 (0)	0.04
Two-dimensional echocardiography			
LA diameter, mm	33.2 ± 6.6	33.1 ± 3.4	0.92
LV end-diastolic diameter, mm	46.3 ± 5.5	47.8 ± 7.1	0.41
LV end-diastolic volume, ml	100.5 ± 28.2	101.2 ± 21.3	0.97
LV end-systolic diameter, mm	29.3 ± 4.4	31.0 ± 4.1	0.58
LV end-systolic volume, ml	34.2 ± 12.0	34.9 ± 11.2	0.88
Interventricular septum, mm	9.1 ± 1.9	9.6 ± 2.0	0.61
LV posterior wall, mm	9.1 ± 0.9	9.4 ± 2.2	0.52
LV ejection fraction, %	66.1 ± 7.6	66.1 ± 7.1	0.89
LV mass index, kg/m^2	97.7 ± 14.6	104.6 ± 33.4	0.44
E/A	1.47 ± 0.50	1.30 ± 0.17	0.14
E/E’	6.3 ± 2.0	5.2 ± 1.8	0.32

Abbreviations: DM = diabetes mellitus, LA = left atrial, LV = left ventricular

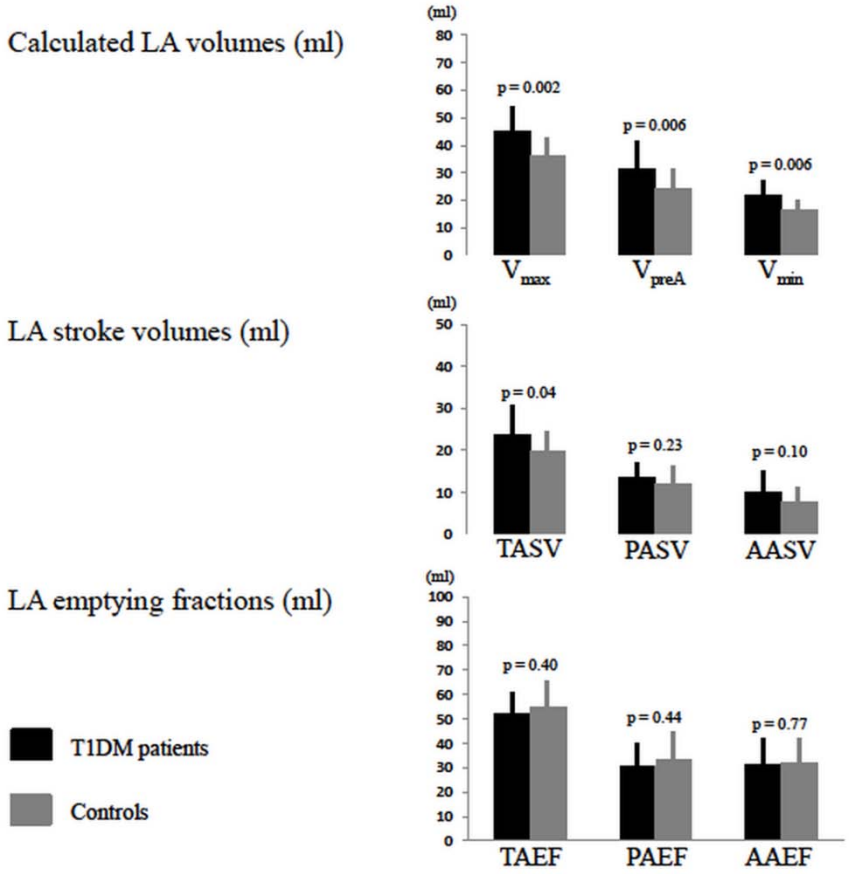

Figure 10. Calculated left atrial volumes and volume-based functional properties (stroke volumes and emptying fractions) are presented in type 1 diabetes mellitus patients and matched healthy controls.
Abbreviations: Vmax – maximum left atrial volume, Vmin – minimum left atrial volume, VpreA - left atrial volume before atrial contraction, TASV – total atrial stroke volume, PASV – passive atrial stroke volume, AASV – active atrial stroke volume, TAEF – total atrial emptying fraction, PAEF – passive atrial emptying fraction, AAEF – active atrial emptying fraction, LA – left atrial, T1DM – type 1 diabetes mellitus

3DSTE-derived peak strain parameters. Global, mean segmental and basal, midatrial and superior segmental peak strain parameters of T1DM patients and control subjects are presented in Figures 11 and 12. Only mean segmental circumferential peak strain showed significant difference between groups (37.3 ± 12.5% vs. 28.9 ± 11.4%, p =0.04). Segmental basal longitudinal (26.8 ± 9.2% vs. 17.3 ± 6.7%, p =0.001) and area (69.1 ± 16.0% vs. 54.4 ± 16.4%, p =0.01) strains were increased, while segmental superior circumferential (33.8 ± 18.5% vs. 17.2 ± 16.8%. p =0.008) and area (71.1 ± 38.8%, vs. 39.7 ± 45.1%, p =0.03) strains and midatrial 3-D strain (-16.8% ± 8.8% vs. -11.2% ± 6.8%, p=0.04) proved to be decreased in T1DM.

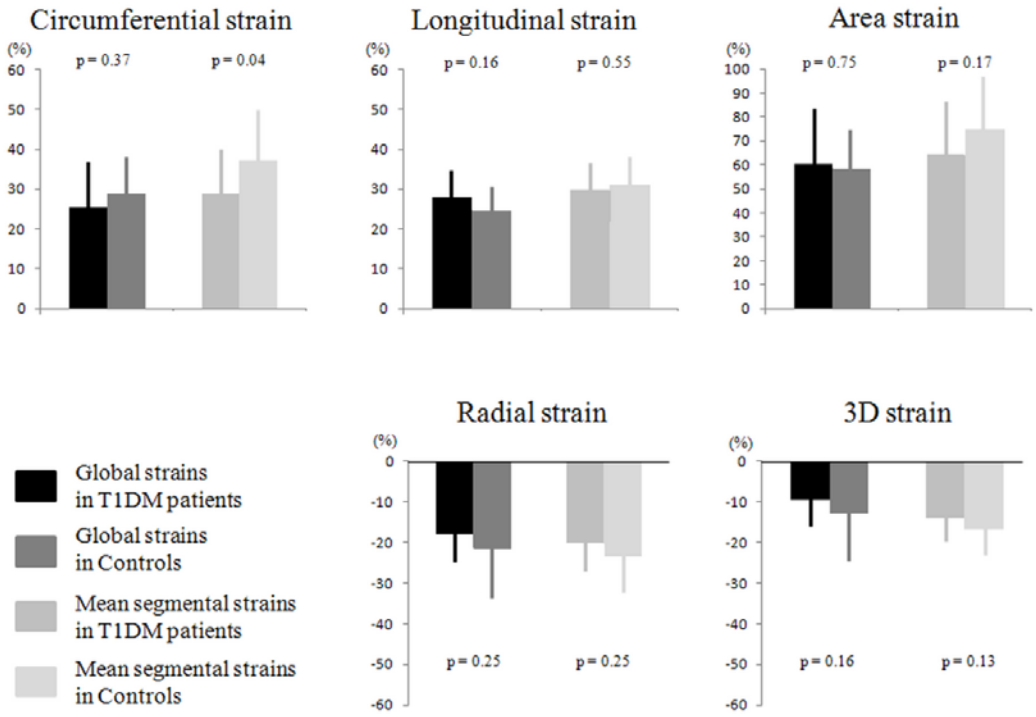

Figure 11. Left atrial global and mean segmental peak circumferential, longitudinal, area, radial and three-dimensional strains are presented in type 1 diabetes mellitus patients and matched healthy controls.
Abbreviation: T1DM – type 1 diabetes mellitus

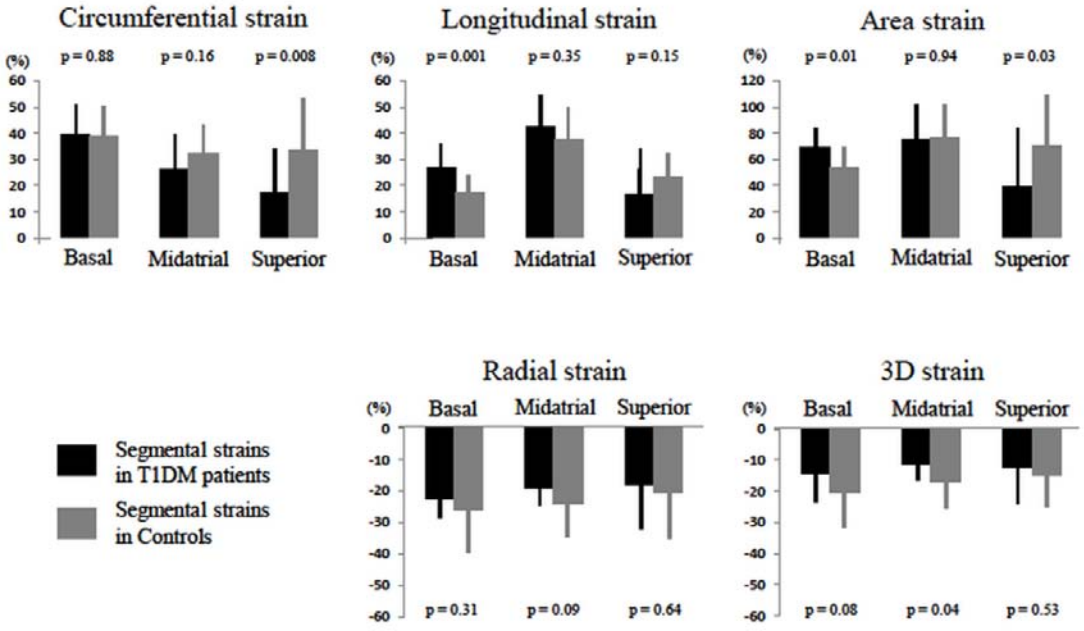

Figure 12. Left atrial segmental basal, midatrial and superior peak circumferential, longitudinal, area, radial and three-dimensional strains are presented in type 1 diabetes mellitus patients and matched healthy controls.
Abbreviation: T1DM – type 1 diabetes mellitus

Reproducible measurements. The mean ± standard deviation difference in values obtained by 2 measurements of the same observer and 2 observers for the measurements of 3DSTE-derived V_{max}, V_{min}, V_{preA}, RS, CS, LS, AS and 3DS together with correlation coefficients are demonstrated in Table 12.

Table 12 Intra- and interobserver variability for the most important parameters in patients with type 1 diabetes mellitus

	Intraobserver agreement		**Interobserver agreement**	
	mean ± SD difference in values obtained by 2 measurements of the same observer	**correlation coefficient between measurements of the same observer**	**mean ± SD difference in values obtained by 2 observers**	**correlation coefficient between independent measurements of 2 observers**
Volumetric data				
V_{max}	0.9 ± 4.7 ml	0.97 (p =0.0001)	1.0 ± 6.4 ml	0.95 (p=0.0001)
V_{min}	-1.1 ± 6.5 ml	0.85 (p =0.0001)	-1.2 ± 7.4 ml	0.83 (p =0.0001)
V_{preA}	0.3 ± 3.7 ml	0.98 (p= 0.0001)	0.2 ± 5.3 ml	0.95 (p =0.0001)
Global strains				
Radial strain	-2.5 ± 11.1%	0.68 (p =0.003)	-0.6 ± 9.6%	0.75 (p =0.0005)
Circumferential strain	3.8 ± 14.8%	0.77 (p =0.0003)	3.6 ± 18.0%	0.73 (p =0.0009)
Longitudinal strain	0.6 ± 8.5%	0.67 (p =0.003)	-2.0 ± 15.7%	0.54 (p =0.02)
Area strain	10.2 ± 37.1%	0.59 (p =0.01)	2.3 ± 38.0%	0.75 (p =0.0005)
3D strain	-1.1 ± 10.4%	0.62 (p =0.008)	1.4 ± 9.5%	0.71 (p =0.001)

Abbreviations: SD = standard deviation, 3D = three-dimensional, V_{max} = maximum left atrial volume, V_{min} = minimum left atrial volume, V_{preA} = left atrial volume before atrial contraction

4.5. Left atrial volumetric and strain analysis in noncompaction cardiomyopathy

Patient population. The present study comprised 12 patients with typical features of NCCM. The diagnosis of NCCM was confirmed in all patients according to the Jenni's criteria (23). Their results were compared to 20 age- and gender-matched healthy controls. Complete 2D Doppler echocardiography and 3DSTE have been performed in all NCCM cases and controls.

Clinical characteristics of patients. Cardiovascular risk factors and medications of NCCM patients and controls are presented in Table 13.

Two-dimensional echocardiographic data. Standard 2D echocardiographic data are summarized in Table 2. Significant (>grade 2) mitral regurgitation could be detected in 4 patients with NCCMP (33%) and in none of controls. Increased LV diameters and volumes, and decreased LVEF could be confirmed in NCCM patients (Table 13).

Three-dimensional speckle-tracking echocardiographic data. Significantly increased LA maximum and minimum volumes and LA volume before atrial contraction could be detected in NCCM patients. Total, passive and active LA emptying fractions were significantly decreased in patients with NCCM (Table 14). Peak global and mean LA segmental strains proved to reduced in NCCM patients as compared to controls (Table 15). Alterations in segmental LA strain parameters in NCCM patients are summarized in Table 16. The number of noncompacted segments (extent of noncompaction) did not correlate with atrial functional properties.

Table 13. Clinical and two-dimensional echocardiographic characteristics of patients with noncompaction cardiomyopathy and of controls

	NCCM patients (n = 12)	Controls (n = 20)	p value
Risk factors			
Age (years)	54.2 ± 15.0	51.9 ± 12.7	0.65
Male gender (%)	5 (42)	12 (60)	0.47
Diabetes mellitus (%)	0 (0)	0 (0)	1.00
Hypertension (%)	5 (42)	0 (0)	0.004
Hypercholesterolaemia (%)	3 (25)	0 (0)	0.04
Medications			
β-blockers (%)	10 (83)	0 (0)	<0.0001
ACE-inhibitors (%)	10 (83)	0 (0)	<0.0001
Diuretics (%)	9 (75)	0 (0)	<0.0001
Two-dimensional echocardiography			
LA diameter (mm)	49.4 ± 8.7	33.0 ± 2.0	<0.0001
LV end-diastolic diameter (mm)	62.7 ± 13.2	47.4 ± 4.3	<0.0001
LV end-diastolic volume (ml)	198.8 ± 89.5	104.6 ± 21.1	0.0001
LV end-systolic diameter (mm)	47.7 ± 15.4	31.0 ± 4.3	0.0001
LV end-systolic volume (ml)	116.2 ± 76.5	37.5 ± 10.3	0.0001
Interventricular septum (mm)	10.1 ± 1.8	9.1 ± 2.0	0.17
LV posterior wall (mm)	9.8 ± 1.4	9.8 ± 2.1	1.00
LV ejection fraction (%)	41.5 ± 17.7	64.0 ± 6.1	<0.0001
E/A	1.6 ± 0.7	1.2 ± 0.1	0.02
Number of noncompacted segments	6.5 ± 1.7	0	-

Abbreviations: ACE: angiotensin-converting enzyme, LA: left atrium, LV: left ventricular, NCCM:noncompaction cardiomyopathy

Table 14. Comparison of three-dimensional speckle-tracking echocardiography-derived left atrial volumetric parameters in patients with noncompaction cardiomyopathy and in controls

	NCCM patients (n=12)	Controls (n=20)	p-value
FR (vps)	23.2 ± 3.6	19.8 ± 0.8	0.0003
Calculated Volumes			
V_{max} (ml)	76.5 ± 26.8	45.3 ± 15.1	0.0002
V_{min} (ml)	56.9 ± 27.3	25.3 ± 15.2	0.0002
$V_{pre}A$ (ml)	67.1 ± 28.2	35.7 ± 16.4	0.0004
Stroke Volumes			
TASV (ml)	19.6 ± 4.8	19.9 ± 6.4	0.89
PASV (ml)	9.5 ± 2.8	9.5 ± 5.3	1.00
AASV (ml)	10.1 ± 5.4	10.3 ± 4.0	0.91
Emptying fractions			
TAEF (%)	29.3 ± 13.1	46.0 ± 13.3	0.002
PAEF (%)	15.1 ± 9.7	22.6 ± 9.0	0.05
AAEF (%)	17.1 ± 8.8	30.7 ± 9.2	0.0003

Abbreviations: AAEF = active atrial emptying fraction, AASV = active atrial stroke volume, FR = frame rate, PSV = passive stroke volume, PAEF = passive atrial emptying fraction, TAEF = total atrial emptying fraction, TASV = total atrial stroke volume, V_{max} = maximum left atrial volume, V_{min} = minimum left atrial volume, $V_{pre}A$ = volume before atrial contraction

Table 15. Comparison of three-dimensional speckle-tracking echocardiography-derived peak global and mean segmental strain parameters in patients with noncompaction cardiomyopathy and in controls

	NCCM patients (n=12)	Controls (n=20)	p-value
Peak global			
RS (%)	-9.3 ± 7.8	-16.8 ± 10.2	0.05
CS (%)	12.8 ± 8.4	26.2 ± 9.2	0.0003
LS (%)	12.8 ± 8.2	22.5 ± 8.5	0.004
3DS (%)	-6.4 ± 5.8	-7.3 ± 12.3	0.81
AS (%)	26.7 ± 18.5	51.6 ± 20.3	0.001
Peak mean segmental			
RS (%)	-12.7 ± 6.9	-19.8 ± 8.0	0.02
CS (%)	16.2 ± 9.1	30.9 ± 11.8	0.0009
LS (%)	15.9 ± 8.9	26.1 ± 7.7	0.002
3DS (%)	-9.3 ± 5.3	-13.7 ± 9.1	0.32
AS (%)	32.4 ± 20.1	58.9 ± 21.3	0.002

Abbreviations: 3DS = three-dimensional strain, AS = area strain, CS = circumferential strain, LS = longitudinal strain, NCCM = noncompaction cardiomyopathy, RS = radial strain

Table 16. Comparison of three-dimensional speckle-tracking echocardiography-derived peak segmental strain parameters in patients with noncompaction cardiomyopathy and in controls

	NCCM patients (n=12)	Controls (n=20)	p-value
RS $_{basal}$ (%)	-9.3 ± 6.7	-23.3 ± 11.4	0.0006
RS $_{mid}$ (%)	-12.8 ± 6.6	-20.6 ± 11.6	0.04
RS $_{apical}$ (%)	-17.9 ± 14.1	-18.8 ± 13.0	0.96
CS $_{basal}$ %)	16.4 ± 12.3	40.6 ± 14.5	<0.0001
CS $_{mid}$ (%)	14.6 ± 9.2	28.8 ± 12.3	0.002
CS $_{apical}$ (%)	19.1 ± 13.8	25.9 ± 16.7	0.24
LS $_{basal}$ (%)	13.0 ± 5.7	19.6 ± 10.8	0.06
LS $_{mid}$ %)	21.9 ± 14.2	35.4 ± 10.2	0.004
LS $_{apical}$ (%)	11.6 ± 8.6	20.9 ± 10.9	0.02
3DS $_{basal}$ (%)	-6.5 ± 4.3	-17.7 ± 10.9	0.002
3DS $_{mid}$ (%)	-9.2 ± 5.2	-13.3 ± 9.7	0.19
3DS $_{apical}$ %)	-13.4 ± 10.2	-12.4 ± 9.0	0.77
AS $_{basal}$ (%)	27.6 ± 19.0	58.9 ± 26.7	0.001
AS $_{mid}$ (%)	37.4 ± 26.8	69.1 ± 27.8	0.004
AS $_{apical}$ (%)	32.7 ± 23.0	54.5 ± 37.5	0.08

Abbreviations: 3DS = three-dimensional strain, AS = area strain, CS = circumferential strain, LS = longitudinal strain, NCCM = noncompaction cardiomyopathy, RS = radial strain

Follow-up. The success rate of follow-up proved to be 100%. During a mean follow-up of 27 ± 1 months, cardiovascular event was found in the anamnaesis of 5 NCCM patients including coronary angiography-proven multivessel disease requiring coronary artery bypass grafting in 2 cases, resynchronisation treatment in 1 case, cardiac decompensation and new-onset atrial fibrillation in 1 case and prosthetic valve implantation due to significant aortic regurgitation and pacemaker implantation due to ventricular arrhythmias in 1 case. 3DSTE-derived atrial volumetric and functional properties in NCCM patients with vs. without events are demonstrated in Tables 17-18.

Table 17. Comparison of three-dimensional speckle-tracking echocardiography-derived left atrial volumetric and volume-based functional parameters in noncompaction cardiomyopathy patients with versus without events during follow-up

	NCCM patients with events (n=5)	**NCCM patients without events (n=7)**	**p-value**
Calculated Volumes			
V_{max} (ml)	92.0 ± 15.0	65.6 ± 28.6	0.09
V_{min} (ml)	73.7 ± 16.2	44.9 ± 28.1	0.07
$V_{pre}A$ (ml)	84.7 ± 16.5	54.5 ± 28.9	0.06
Stroke Volumes			
TASV (ml)	18.4 ± 5.7	20.5 ± 4.2	0.47
PASV (ml)	7.3 ± 2.8	11.0 ± 1.5	0.01
AASV (ml)	11.0 ± 6.4	9.5 ± 5.0	0.65
Emptying fractions			
TAEF (%)	20.3 ± 6.3	35.7 ± 13.0	0.04
PAEF (%)	8.3 ± 4.0	20.0 ± 9.7	0.03
AAEF (%)	13.0 ± 6.9	20.1 ± 9.3	0.18

Abbreviations: AAEF = active atrial emptying fraction, AASV = active atrial stroke volume, NCCM = noncompaction cardiomyopathy, PAEF = passive atrial emptying fraction, PASV = passive stroke volume, RS = radial strain, TAEF = total atrial emptying fraction, TASV = total atrial stroke volume, V_{max} = maximum left atrial volume, V_{min} = minimum left atrial volume, $V_{pre}A$ = volume before atrial contraction

Table 18. Comparison of three-dimensional speckle-tracking echocardiography-derived left atrial strain parameters in noncompaction cardiomyopathy patients with versus without events during follow-up

	NCCM patients with events (n=5)	NCCM patients without events (n=7)	p-value
Peak global strains			
RS (%)	5.8 ± 3.9	11.9 ± 9.1	0.19
LS (%)	7.1 ± 3.9	16.9 ± 8.2	0.03
CS (%)	9.3 ± 8.6	15.3 ± 8.0	0.24
3DS (%)	4.6 ± 3.2	7.7 ± 7.0	0.38
AS (%)	15.2 ± 13.8	34.9 ± 17.6	0.06
Mean segmental strains			
RS (%)	9.5 ± 2.8	15.1 ± 8.2	0.18
LS (%)	9.1 ± 3.3	20.8 ± 8.4	0.01
CS (%)	11.3 ± 8.1	19.8 ± 8.6	0.12
3DS (%)	7.3 ± 3.2	10.7 ± 6.2	0.29
AS (%)	19.3 ± 13.6	41.8 ± 19.2	0.05

Abbreviations: AS = area strain, CS = circumferential strain, LS = longitudinal strain, NCCM = noncompaction cardiomyopathy, RS = radial strain, 3DS = three-dimensional strain

5. Discussion

5.1. Relationships between right atrial and left ventricular size and function in healthy subjects

In our study, LVEF showed relationship both with systolic and diastolic RA volumes. While LVEF did not correlate with RA stoke volumes and emptying fractions, correlations could be detected between LVEF and diastolic AS measured at atrial contraction. RA volumes respecting cardiac cycle showed correlations only with LV-ESD and LV-ESV, similar correlations with end-diastolic parameters could not be detected. Relationship could be

demonstrated between LV-ESD and LV-ESV and certain diastolic RA functional parameters at atrial contraction. Similarly, relationship could be demonstrated between LV-EDD and systolic and diastolic RA strain parameters.

It is well known that to maintain normal circulation aligned movement of the atria and ventricles is essential (1). Recent imaging cardiovascular techniques seem to be suitable not only for quantitative detection of changes in cardiac chamber sizes but for calculation of different functional parameters. Calculation of LV dimensions (diameter, volume) and function (LV fractional shortening, LVEF) is a part of the daily routine examination by M-mode and 2D echocardiography (2,30). There are further opportunities for more detailed analysis due to presence of complementary methodologies including Doppler, tissue Doppler, 2DSTE, volumetric RT3DE and strain-based 3DSTE (30).

Unfortunately routine 2D echocardiography suffers in featuring RA dimensions, volumes and function (31,32). RA (similarly to LA) has a complex motion during the heart cycle, working as a reservoir in systole, while conduit and actively contracting heart chamber in diastole (32). 3DSTE is a new methodology with which 3D model of the RA could be created by digitally acquired RA-focused 3D databases. Due to ECG gating changes in volumetric and functional parameters could be analysed respecting the heart cycle. However, there were no previous 3DSTE studies, in which RA and LV functional relationship was examined in healthy subjects.

The number of studies related to recent echocardiographic examination of RA volumes and functional parameters is limited. RT3DE was found to be a reliable non-invasive methodology for assessment of RA volume changes respecting the heart cycle, and RA volumes changes were confirmed by RT3DE in different disorders (33,34). 2DSTE was also found to be a tool for quantitative characterization of RA wall motion as confirmed in several papers (35,36). The newly developed 3DSTE overcome technical difficulties which could arise during 2DSTE (for instance inaccuracy in the evaluation of motions which leave 2D plane), because the whole imaging (virtual 3D cast of RA) is based on 3D tracking of speckles (acoustic echo samples) (3-5,26,27). The other important advantage of the method is that not only changes in chamber volumes, but strain, rotational and dyssynchrony parameters could be measured at the same time from the same 3D cast (4,26,27).

The present study aimed to highlight attentation on the fact that with this new methodology detailed analysis of RA is possible via volumetric and functional measurements during a simple ultrasound examination of the heart. Results have confirmed relationships between above mentioned RA and LV morphological and functional parameters, which could

help understanding physiologic contexts during heart cycle. However, further studies are warranted in larger patient populations to confirm our results and to clarify the role of other factors including valves' sizes and functional parameters, as emerged from previous studies.

Study limitations. One the important limitations is that RA appendage, caval veins and sinus coronarius were excluded from analyses. The present study aimed to compare 3DSTE-derived RA volumes and functional parameters and 2D echocardiographic LV data in healthy subjects. The other heart chambers and valves participating in maintaining circulation were not examined in this study. 3DSTE examination of LV, RV and LA and 2D echocardiographic analysis of the RA were even not aimed to be assessed in this particular study. 3DSTE-derived image quality is much worse than that could be experienced during 2D echocardiography, which could theoretically affect results. During performing 3D cast of the RA a methodology validated for LA was used (6,8,9). This could be considered when interpreting our results. Finally, although 3DSTE is suitable for measuring rotational, twist and synchronicity features of a certain heart chamber, it was not aimed to be examined.

5.2. Correlations between left atrial ejection force and left atrial strain and volume-based functional properties in healthy subjects

The newly developed 3DSTE is a non-invasive imaging methodology with ability for chamber quantifications based on block-matching algorithm of the myocardial speckles of the endocardial border during their frame-to-frame motion (4,26,27). As mentioned before, usefulness of 3DSTE for LA volumetric assessments has been demonstrated and validated by 2D echocardiography (9), 2DSTE (8), RT3DE (6) and computer tomography (8). Moreover, 3DSTE-derived LA strain measurements have also been demonstrated (10-12) and validated before by 2DSTE (11).

In most of cases, volumetric and strain assessments could be performed simultaneously using the same 3D model of the LA. However, there is a third way to characterize LA function during the same examination measuring LAEFO, the force exerted by the LA to accelerate blood into the LV during atrial systole. LAEFO is based on classic Newtonian mechanics and is a potential useful index for assessing atrial contribution to diastolic performance (28). Over 2D imaging both 3D echocardiographic techniques, RT3DE (14,21,37) and 3DSTE (13) have been demonstrated to be practicable in assessing LAEFO

using Doppler-derived mitral inflow A velocity. However, to the best of authors' knowledge this is the first time to examine whether correlations exist between 3DSTE-derived LAEFO and LA volume-based and strain funtional properties respecting cardiac systolic and diastolic functions in healthy subjects.

In a recently published paper from the MAGYAR-Healthy Study, 3DSTE seemed to be feasible in detection of cyclic changes in LA volumes and calculation of its functional properties was comparable to 2D echocardiography (9). Good correlations were found between both techniques for LA volumetric data and volume-based functional properties. Moreover, excellent intra- and interobserver agreements could be demonstrated for 3DSTE-derived volumetric and strain data (9). Results of the present study extended our knowledge demonstrating capability of 3DSTE in reproducible assessment of MAD and MAA allowing simple calculation of LAEFO, as well.

The study reported here is the first to demonstrate correlations between LAEFO and 3DSTE-derived volume-based and strain parameters featuring systolic LA reservoir and late diastolic LA booster pump phases calculated from the same 3D model of the LA. No relationships could be demonstrated between LAEFO and functional properties of early diastole (LA conduit function). The results of the present study could higlight our attention on several facts. Firstly, 3DSTE seems to be a simple, non-invasive technology with which complex evaluation of the LA function could be done. All functions of LA including systolic reservoir, early diastolic conduit and late diastolic booster pump (or active contraction) phases could be assessed at the same time by a complex way. Secondly, several volume-based and strain parameters over LAEFO could be calculated from the same 3D model of the LA. The measurement of LAEFO requires more data including MAD or MAA and pulsed Doppler-derived mitral inflow A wave. Thirdly, significant correlations could be demonstrated between these functional properties, as demonstrated before. However, further validation studies with other imaging methodologies are warranted to confirm our findings. Moreover, other studies should focus on deeper insights on atrial (patho)physiology, especially in different cardiovascular disorders using all the methodologies detailed above.

Limitation section. In agreement with available literature, LA appendage and pulmonary veins were excluded from evaluations. Despite most of patients had far from optimal image quality due to low temporal and spatial resolutions, none of them were excluded from the analyses, but could theoretically affect results. Only a limited number of healthy volunteers from a single center were examined and measurements were provided by a single observer.

Although 3DSTE seems to be an applicable technique for non-invasive estimation of LA volumes and functional properties, more comparative and validation studies with other methodologies are warranted. At this moment 3DSTE-derived normal strain reference values has not been described and the results of the present study were somewhat different as compared to that of previous findings. It could be explained by methodological differences, but the effect of the age and other factors could also not be excluded (10,28,37,38). It is known that LA function could be deteriorated in different arrhytmologic disorders like in atrial fibrillation. However, all of the studied healthy subjects were in sinus rhythm. Theoretically higher grade of MR could affect LA function. However, none of the healthy subjects had ≥ grade 1MR. Quantification of LV strains and rotational parameters by 3DSTE was not aimed in the present study.

5.3. Correlations between left atrial functional parameters and aortic stiffness in healthy subjects

To the best of authors' knowledge this is the first study in which correlations could be demonstrated between echocardiographic aortic elastic properties and 3DSTE-derived LA functional parameters in healthy subjects. 3DSTE has been found to be feasible for non-invasive quantification of LA volumes and functional properties allowing complex evaluation of LA phasic function during cardiac cycle which includes (3,39):

[1] Reservoir function (LA inflow during LA systole)

[2] Conduit function (LA passive emptying during LV relaxation and diastasis, when blood transiting from the pulmonary veins to the LV during early diastole)

[3] Active contraction or booster pump function (LA active emptying, when LA works like an active contractile chamber that augments LV filling in late diastole).

There are several ways for functional assessment of LA including calculation of volume-based and strain parameters by 3DSTE as demonstrated before (6,8-13). With these parameters detailed characterization of all three LA functions possible:

[1] *Reservoir function* by total atrial SV and total atrial EF together with global and mean segmental peak strain parameters,

[2] *Conduit function* by passive atrial SV and passive atrial EF, and

[3] *Active contraction (booster pump)* by active atrial SV and active atrial EF together with global and mean segmental strain parameters at atrial contraction.

It is known that due to large number of collagens and filaments, the normal aorta is working as an elastic artery. As a physiologic consequence of the reduction of aortic buffering (Windkessel) function, SBP increases and DBP decreases leading to increased LV afterload and impaired LV relaxation (40). In the present study most of functional LA parameters showing correlations with aortic elastic properties are characteristics of atrial booster pump function reflecting magnitude and timing of atrial contractility but is dependent on the degree of venous return, LV end-diastolic pressures and LV systolic reserve (3). Moreover, correlations were found between aortic elasticity and characteristics of LA reservoir and conduit functions, as well. Because of the close interplay between LA, LV remodeling and diastolic function, the relationship is not suprising. However, in the present study detailed analysis could be demonstrated between echocardiographic aortic elastic properties and all the LA phasic functions by 3DSTE-derived volume-based and strain parameters even in healthy subjects.

Limitation section. Over previously mentioned limitations it should be considered that the blood pressure in the brachial artery and ascending aorta may be different which could theoretically affect our results. However, the presented non-invasive imaging technique has been validated against invasive methods in the evaluation of aortic stiffness parameters (25,40).

5.4. Complex evaluation of left atrial dysfunction in patients with type 1 diabetes mellitus

The present study features a novel aspect of early LA remodeling in T1DM patients with the aid of 3DSTE. Changes in LA volumes and functional properties respecting cardiac cycle suggesting LA remodeling could highlight our attention on the importance of early diagnosis, treatment and follow-up of young patients with T1DM who have not yet overt cardiovascular disease.

In the present study total atrial SV was found to be increased together decreased mean segmental circumferential peak strain in T1DM patients. Segmental analysis have revealed that basal longitudinal and area strains are increased, while superior circumferential and area strains are decreased in T1DM suggesting augmented basal and reduced superior LA deformations in reservoir phase of the LA function. However, alterations in conduit and active contraction phases of LA function could not be confirmed by 3DSTE in this patient subset.

Our results are only partially in agreement with previous findings. Acar *et al.* found decreased LA passive EF and increased LA active emptying volume and LA active EF in T1DM patients (41). In another study, during cold pressor test, isovolumic relaxation time increased, peak early LV filling velocity (E) decreased, E deceleration time decreased and LA contribution (A) increased significantly in T1DM. A marked increase in LA ejection force was also seen in this study. This LA hyperfunction was hypothesized to be due to reduced size of the LV combined with incipient autonomic neuropathy (42). Peterson *et al.* found that T1DM is related to A wave velocity, late myocardial velocity (Am global), LA ejection fraction and LA systolic ejection fraction (43).

The prevalence of hypertension was frequent in our diabetic patient population, which is a common finding in T1DM. In a recent 2DSTE study, hypertension was found to be associated with impaired LA function even before LA enlargement develops and after LV remodeling is accounted for (44). Badran *et al.* found that in hypertension LA conduit function is chiefly affected and LA dysfunction is linked to a more advanced disease (45).

The real mechanism behind the LA volumetric and functional alterations and LA remodeling is not yet known in T1DM. However, diabetes-related hormonal changes, necrosis, progressive fibrosis, haemodynamic reasons and the effect of diastolic dysfunction etc. could not be excluded. Moreover, the effects of diabetes-related hypertension should also be considered.

Study Limitations. Over previous limitations it should be considered that the present single-center study covered a small number of T1DM patients, which should be considered as the most important limitation. Moreover, one quarter of T1DM patients had treated hypertension and/or hypercholesterolaemia and HbA1c of T1DM patients was significantly increased, which could theoretically affect results.

5.5. Left atrial volumetric and strain analysis in noncompaction cardiomyopathy

To the best of authors' knowledge this is the first study in which LA function was assessed by 3DSTE in a series of patients with NCCM and compared to matched controls. Increased LA volumes, reduced LA emptying fractions and peak LA strain parameters could be demonstrated in NCCM.

Cardiomyopathies are frequently associated with volumetric and functional deteriorations of different heart chambers (46-48). However, relatively low number of studies

are available, in which LA (dys)function was investigated in NCCM. In a recent RT3DE study, LA ejection force was found to be increased in NCCM as compared to controls (13,21). In the present study, significantly reduced AAEF could be demonstrated during LA contraction. Moreover, all calculated LA volumes proved to be increased, while LA emptying fractions respecting cardiac cycle were decreased in NCCM demonstrating significant alterations in all LA functions. During strain analysis certain peak global and mean segmental strain parameters showed reductions in NCCM patients confirming changes in LA reservoir function.

Limitation section. Over above mentioned limitations it should be taken into consideration that results of a relatively small number of NCCM patients were analysed. However, it should be considered that this was a single-centre experience and NCCM is a relative rare disorder. Some NCCM patients showed higher grade mitral regurgitation. This could affect our results.

6. Conclusions (new observations)

Relationships could be demonstrated between three-dimensional speckle tracking echocardiography-derived right atrial and two-dimensional echocardiography-derived left ventricular volumetric and functional parameters in healthy subjects.

Complex left atrial functional assessment could be provided by three-dimensional speckle tracking echocardiography including calculation of left atrial ejection force and volume-based and strain functional properties with significant correlations between these parameters.

Correlations exist between three-dimensional speckle tracking echocardiography-derived functional left atrial parameters and echocardiographic aortic elastic properties in healthy subjects.

Three-dimensional speckle tracking echocardiography-derived volumetric and strain analysis confirmed alterations in left atrial function in young patients with type 1 diabetes mellitus suggesting early remodeling of the left atrium before other cardiovascular alterations occur.

Significantly increased left atrial volumes and impaired left atrial function could be demonstrated in noncompaction cardiomyopathy by three-dimensional speckle tracking echocardiography.

7. References

1. Feigenbaum H. Echocardiography. 5ht Edition, Lea et Febiger, Philadelphia, 1993.
2. Teichholz LE, Cohen MV, Sonnenblick EH, Gorlin R. Study of the left ventriculat geometry and function by B-scan ultrasonography in patients with and without asynergy. N Engl J Med 1974; 291: 1220-1226.
3. Hoit BD. Left atrial size and function: role in prognosis. J Am Coll Cardiol 2014; 63: 493-505.
4. Nemes A, Kalapos A, Domsik P, Forster T. Three-dimensional speckle-tracking echocardiography -- a further step in non-invasive three-dimensional cardiac imaging. Orv Hetil 2012; 153: 1570-1577.
5. Nemes A, Forster T. Assessment of left atrial size and function -- from M-mode to 3D speckle-tracking echocardiography. Orv Hetil 2014; 155: 1624-1631.
6. Kleijn SA, Aly MF, Terwee CB, van Rossum AC, Kamp O. Comparison between direct volumetric and speckle tracking methodologies for left ventricular and left atrial chamber quantification by three-dimensional echocardiography. Am J Cardiol 2011; 108: 1038-1044.
7. Nemes A, Havasi K, Domsik P, Kalapos A, Forster T. Evaluation of right atrial dysfunction in patients with corrected tetralogy of Fallot using 3D speckle-tracking echocardiography. Insights from the CSONGRAD Registry and MAGYAR-Path Study. Herz 2015; 40: 980-988.
8. Nagaya M, Kawasaki M, Tanaka R, Onishi N, Sato N, Ono K, Watanabe T, Minatoguchi S, Miwa H, Goto Y, Hirose T, Arai M, Noda T, Watanabe S, Minatoguchi S. Quantitative validation of left atrial structure and function by two-dimensional and three-dimensional speckle tracking echocardiography: A comparative study with three-dimensional computed tomography. J Cardiol 2013; 62: 188–194.
9. Nemes A, Domsik P, Kalapos A, Lengyel C, Orosz A, Forster T. Comparison of three-dimensional speckle-tracking echocardiography and two-dimensional echocardiography for evaluation of left atrial size and function in healthy volunteers (Results from the MAGYAR-Healthy Study). Echocardiography 2014; 31: 865-871.
10. Domsik P, Kalapos A, Chadaide S, Sepp R, Hausinger P, Forster T, Nemes A. Three-dimensional speckle tracking echocardiography allows detailed evaluation of left atrial

function in hypertrophic cardiomyopathy - insights from the MAGYAR-Path Study. Echocardiography 2014; 31: 1245-1252.

11. Mochizuki A, Yuda S, Oi Y, Kawamukai M, Nishida J, Kouzu H, Muranaka A, Kokubu N, Shimoshige S, Hashimoto A, Tsuchihashi K, Watanabe N, Miura T. Assessment of left atrial deformation and synchrony by three-dimensional speckle-tracking echocardiography: comparative studies in healthy subjects and patients with atrial fibrillation. J Am Soc Echocardiogr 2013; 26: 165-174.
12. Chadaide S, Domsik P, Kalapos A, Saghy L, Forster T, Nemes A. Three-dimensional speckle tracking echocardiography–derived left atrial strain parameters are reduced in patients with atrial fibrillation (Results from the MAGYAR-Path Study). Echocardiography 2013; 30: 1078-1083.
13. Nemes A, Hausinger P, Kalapos A, Domsik P, Forster T. Alternative ways to assess left atrial function in noncompaction cardiomyopathy by three-dimensional speckle-tracking echocardiography: (a case from the MAGYAR-Path study). Int J Cardiol 2012; 158: 105-107.
14. Anwar AM, Soliman OI, Geleijnse ML, Michels M, Vletter WB, Nemes A, ten Cate FJ. Assessment of left atrial ejection force in hypertrophic cardiomyopathy using real-time three-dimensional echocardiography. J Am Soc Echocardiogr 2007; 20: 744-748.
15. Chae CU, Pfeffer MA, Glynn RJ, Mitchell GF, Taylor JO, Hennekens CH. Increased pulse pressure and risk of heart failure in the elderly. JAMA 1999; 281: 634-639.
16. Cioffi G, Mureddu GF, Stefenelli C, Simine G: Relationship between left ventricular geometry and left atrial size and function in patients with systemic hypertension. J Hypertens 2004; 22: 1589-1596.
17. Lantelme P, Laurent S, Besnard C, Bricca G, Vincent M, Legedz L, Milon H. Arterial stiffness is associated with left atrial size in hypertensive patients. Arch Cardiovasc Dis 2008; 101: 35–40.
18. Slim IB. Cardiovascular risk in type 1 diabetes mellitus. Indian J Endocrinol Metab 2013; 17: S7-S13.
19. Raev DC. Which left ventricular function is impaired earlier in the evolution of diabetic cardiomyopathy? An echocardiographic study of young type I diabetic patients. Diabetes Care 1994; 17: 633-639.
20. Jenni R, Oechslin E, Schneider J, Attenhofer Jost C, Kaufmann PA. Echocardiographic and pathoanatomical characteristics of isolated left ventricular non-

compaction: A step towards classification as a distinct cardiomyopathy. Heart 2001; 86: 666-671.

21. Nemes A, Anwar AM, Caliskan K, Soliman OI, van Dalen BM, Geleijnse ML, ten Cate FJ. Evaluation of left atrial systolic function in noncompaction cardiomyopathy by real-time three-dimensional echocardiography. Int J Cardiovasc Imaging 2008; 24: 237-242.
22. World Medical Association Declaration of Helsinki, Ethical Principles for Medical Research Involving Human Subjects. http:// www.wma.net/en/30publications/10policies/b3/index.html,
23. Nagueh SF, Appleton CP, Gillebert TC, Marino PN, Oh JK, Smiseth OA, Waggoner AD, Flachskampf FA, Pellikka PA, Evangelisa A. Recommendation for the evaluation of left ventricular diastolic function by echocardiography. Eur J Echocardiogr 2009; 10: 165-193.
24. Nemes A, Geleijnse ML, Forster T, Soliman OI, Ten Cate FJ, Csanady M. Echocardiographic evaluation and clinical implications of aortic stiffness and coronary flow reserve and their relation. Clin Cardiol 2008; 31: 304–309.
25. Stefanadis C, Stratos C, Boudoulas H, Kourouklis C, Toutouzas P. Distensibility of the ascending aorta: comparison of invasive and non-invasive techniques in healthy men and in men with coronary artery disease. Eur Heart J 1990; 11: 990–996.
26. Ammar KA, Paterick TE, Khandheria BK, Jan MF, Kramer C, Umland MM, Tercius AJ, Baratta L, Tajik AJ. Myocardial mechanics: understanding and applying three-dimensional speckle tracking echocardiography in clinical practice. Echocardiography 2012; 29: 861–872.
27. Urbano-Moral JA, Patel AR, Maron MS, Arias-Godinez JA, Pandian NG. Three-dimensional speckle-tracking echocardiography: Methodological aspects and clinical potential. Echocardiography 2012; 29: 997-1010.
28. Manning WJ, Silverman DI, Katz SE, Douglas PS. Atrial ejection force: a noninvasive assessment of atrial systolic function. J Am Coll Cardiol 1993; 22: 221–225.
29. Bland JM, Altman DG: Statistical methods for assessing agreement between two methods of clinical measurement. Lancet 1986; 1: 307-310.
30. Nemes A, Forster T. Recent echocardiographic examination of the left ventricle – from M-mode to 3D speckle-tracking imaging. Orv Hetil 2015; 156: 1723-1740.
31. Baur LH. Right atrial function: still underestimated in clinical cardiology. Int J Cardiovasc Imaging 2008; 24: 711-712.

32. Müller H, Burri H, Lerch R. Evaluation of right atrial size in patients with atrial arrhytmias: comparison of 2D versus real time 3D echocardiography. Echocardiography 2008; 25: 617-623.
33. Tadic M., Cuspidi C., Suzic-Lazic J, Andric A, Stojcevski B, Ivanovic B, Hot S, Scepanovic R, Celic V. Is there a relationship between right-ventricular and right atrial mechanics and functional capacity in hypertensive patients? J Hypertens 2014; 32: 929-937.
34. Müller H, Reverdin S, Burri H, Shah D, Lerch R. Measurement of left and right atrial volume in patients undergoing ablation for atrial arrhythmias: comparison of a manual versus semiautomatic algorithm of real time 3D echocardiography. Echocardiography 2014; 31: 499-507.
35. Durmus E, Sunbul M, Tigen K, Kivrak T, Ozen G, Sari I, Direskeneli H, Basaran Y. Right ventricular and atrial functions in systemic sclerosis patients without pulmonary hypertension. Speckle-tracking echocardiographic study. Herz 2015; 40: 709-715.
36. Moustafa S, Zuhairy H, Youssef MA, Alvarez N, Connelly MS, Prieur T, Mookdam F. Right and Left Atrial Dissimilarities in Normal Subjects Explored by Speckle Tracking Echocardiography. Echocardiography 2015; 32: 1392-1399.
37. Zhong L, Tan, LK, Finn CJ, Ghista D, Liew R, Ding ZP. Effects of age and gender on left atrial ejection force and volume from real-time three-dimensional echocardiography. Ann Acad Med Singapore 2012; 41: 161-169.
38. Blume GG, Mcleod CJ, Barnes ME, Seward JB, Pellikka PA, Bastiansen PM, Tsang TS. Left atrial function: physiology, assessment, and clinical implications. Eur J Echocardiogr 2011; 12: 421-430.
39. Barbier P, Solomon, SB, Schiller NB, Glantz SA. Left atrial relaxation and left ventricular systolic function determine left atrial reservoir function. Circulation 1999; 100: 427-436.
40. Belz GG. Elastic properties and Windkessel function of the human aorta. Cardiovasc Drugs Ther 1995; 9: 73–83.
41. Acar G, Akcay A, Sokmen A, Ozkaya M, Guler E, Sokmen G, Kaya H, Nacar AB, Tuncer C. Assessment of atrial electromechanical delay, diastolic functions, and left atrial mechanical functions in patients with type 1 diabetes mellitus. J Am Soc Echocardiogr 2009; 22: 732-738.

42. Gøtzsche O, Darwish A, Hansen LP, Gøtzsche L. Abnormal left ventricular diastolic function during cold pressor test in uncomplicated insulin-dependent diabetes mellitus. Clin Sci (Lond) 1995; 89: 461-465.
43. Peterson LR, Waggoner AD, de las Fuentes L, Schechtman KB, McGill JB, Gropler RJ, Dávila-Román VG. Alterations in left ventricular structure and function in type-1 diabetics: A focus on left atrial contribution to function. J Am Soc Echocardiogr 2006; 19: 749-755.
44. Xu TY, Sun JP, Lee AP, Yang XS, Ji L, Zhang Z, Li Y, Yu CM, Wang JG. Left atrial function as assessed by speckle-tracking echocardiography in hypertension. Medicine (Baltimore) 2015; 94: e526.
45. Badran HM, Faheem N, Elnoamany MF, Kenawy A, Yacoub M. Characterization of left atrial mechanics in hypertrophic cardiomyopathy and essential hypertension using vector velocity imaging. Echocardiography 2015; 32: 1527-1538.
46. Mornos C, Manolis AJ, Cozma D, Kouremenos N, Zacharopoulou I, Ionac A. The value of left ventricular global longitudinal strain assessed by three-dimensional strain imaging in the early detection of anthracyclinemediated cardiotoxicity. Hellenic J Cardiol 2014; 55: 235-244.
47. Trachanas K, Sideris S, Aggeli C, Poulidakis E, Gatzoulis K, Tousoulis D, Kallikazaros I. Diabetic cardiomyopathy: from pathophysiology to treatment. Hellenic J Cardiol 2014; 55: 411-421.
48. Doesch C, Schimpf R, Haneder S, Borggrefe M, Papavassiliu T. Patient with hypertrophic cardiomyopathy with apical aneurysm and thrombus presenting with progressive congestive heart failure. Hellenic J Cardiol 2015; 56: 258-259.

8. Acknowledgements

The studies reported in this work were performed at the 2nd Department of Medicine and Cardiology Center, Medical Faculty, Albert Szent-Györgyi Clinical Center, University of Szeged, Hungary.

First of all I express my heartfelt gratiutude to Prof. Dr. Attila Nemes for his continuous support during my work, who was my tutor and scientific adviser. Without his support and encouragement this thesis would have not been performed.

I would like to thank very much also Prof. Dr. Tamás Forster, the head of the 2nd Department of Medicine and Cardiology Center, who supported me in my work.

I would like to say thank to all co-authors, Dr. Péter Domsik, Dr. Anita Kalapos, Dr. Csaba Lengyel, Dr. Andrea Orosz and Dr. Tamás T. Várkonyi.

I can also thank to all of my colleagues as well as nurses, assistants and all the members of the Institute.

Photocopies of essential publications